PLEASURE AND PAIN: NUCLEUS ACCUMBENS FUNCTIONAL ARCHITECTURE IN ACUTE AND CHRONIC PAIN

by

Adam Sunavsky

Submitted in partial fulfillment of the requirements for
the degree of Master of Science

at

Dalhousie University
Halifax, Nova Scotia
May 2022

Dedication

This thesis is dedicated to my family, both in Slovakia and Canada. Your love and zest give me the inspiration to do challenging things.

Table of Contents

List of Tables

List of Figures

Abstract

The nucleus accumbens (NAc) is a heterogenous hub involved in the motivational salience of rewarding and aversive stimuli, and in the aetiology of chronic back pain (CBP). Its role in responding to varying threats and noxious stimuli, as well as intrinsic differences in NAc subregion (shell and core) connectivity between healthy controls (HC) and CBP, remain elusive. The first part examines NAc activation to different noxious stimuli after uncertain, low, and high threat cues in 35 HC using task-fMRI. The NAc core preferentially activated to uncertain threats and to violations between expectations and reality. The second part elucidates reproducible NAc subregion connectivity differences between 75 CBP and 71 HC using rest-fMRI. CBP patients had NAc hyperconnectivity to prefrontal regions (NAc-dorsolateral prefrontal cortex) and hypoconnectivity to language/memory and salience regions. This thesis implicates the NAc as a major hub in aversive responding and highlights specific connections for CBP diagnostics and therapeutics.

List of Abbreviations Used

ACC	Anterior cingulate cortex
ACCsg	Subgenual anterior cingulate cortex
ACCrm	Rostral anterior cingulate mid-posterior
ACCrp	Rostral anterior cingulate posterior
AFNI	Analysis of Functional NeuroImages
aIC	Anterior insular cortex
Amyg	Amygdala
ANCOVA	Analysis of covariance
ANOVA	Analysis of variance
AUC	Area under the curve
BDI	Beck Depression Inventory-II
BPI	Brief Pain Inventory
BOLD	Blood oxygenation level dependent
CBP	Chronic back pain
Cingp	Posterior cingulate gyrus
CP	Chronic pain
dINSa	Dorsal anterior insula
dlPFC	Dorsolateral prefrontal cortex
DMN	Default Mode Network
dmPFCa	Dorsomedial prefrontal cortex anterior division
dmPFCp	Dorsomedial prefrontal cortex posterior division
DVARS	Difference of volume N to N+1
FD	Framewise displacement
FDR	False discovery rate
FFMQ	Five-facet Mindfulness Questionnaire
fMRI	Functional magnetic resonance imaging
HC	Healthy controls
Hipp	Hippocampus
IASP	International Association for the Study of Pain
MNI	Montreal Neurological Institute

mPFC	Medial prefrontal cortex
MQS	Medication Quantification Scale
MRI	Magnetic resonance imaging
MTGa	Middle temporal gyrus, anterior division
NAc	Nucleus accumbens
NRS	Numerical rating scale
NPS	Neuropathic Pain Scale
PAG	Periaqueductal grey
PCS	Pain Catastrophizing Scale
rACC	Rostral anterior cingulate cortex
ROC	Receiver operator curve
ROI	Region of interest
rsFC	Resting-state functional connectivity
RSN	Resting-state network
SBP	Subacute back pain
SEM	Standard error of the mean
STAI	State-Trait Anxiety Inventory
vmPFC	Ventromedial prefrontal cortex

Acknowledgements

I started my Master's degree in the midst of the COVID-19 pandemic, with so many uncertainties. Now, I am grateful to say that I have finished stronger, not only as a scientist but also as a person. I could not have done this without the unwavering help from my supervisor, colleagues, friends, and family.

Dr. Javeria Ali Hashmi, thank you for being there through the uncertainty and guiding me with your knowledge, experience, and mentorship. Your excitement and curiosity for research and discovery is infectious, it inspires me to bring this mindset to my future endeavours. Our conversations on absurdism and the meaning of life remind me to keep the big picture in mind but have both feet on the ground. I hope to someday come close to becoming the modest yet powerful leader that you are. I could not have asked for a better supervisor to guide me through this journey.

To the members of my supervisory committee, Dr. Kazue Semba, Dr. Christian Lehmann, and Dr. Steven Beyea, thank you for your feedback throughout my journey and for making my project stronger. I appreciate your areas of expertise and encouragement during the busy moments of my thesis. Dr. Aaron Newman, thank you for agreeing to be my external reviewer so quickly!

To my labmates, Jason and Jennika, thank you for your countless hours you spent helping me troubleshoot Matlab issues, and with data collection. As well, thank you to Guillermo, Meenakshi, Veronika, and Tatiana for helping me in innumerable ways, including keeping a positive vibe in our lab! I appreciate all of you!

Finally, to my family and friends, thank you for your love, support, and guidance, without you my life would be without purpose. You give me the resolve and strength to be a better person and the courage to push forward through uncertainty and adversity. Thank you, thank you, thank you.

CHAPTER 1. Introduction

1.1. A Brief History of Pain

1.1.1. Overview

Pain is a multimodal sensation, often caused by suprathreshold noxious stimuli. Traditionally, pain has been viewed as a reaction to sensory insults, when tissue damage occurs (Mountcastle & Darian-Smith, 1968). However, pain can also be present in the absence of noxious stimuli, such as during phantom limb pain or when there is probability of tissue damage. The International Association for the Study of Pain (IASP) defines pain as "an unpleasant sensory and emotional experience associated with, or resembling that associated with, actual or potential tissue damage" (Raja et al., 2020). The multidimensional nature of pain necessitates a review of past and current theories of pain.

1.1.2. Historical Theories of Pain

While theories underlying mechanisms of pain perception date back millennia (Perl, 2007), the most influential ones to date are the Intensity, Specificity, Pattern, and Gate Control Theories of Pain (Moayedi & Davis, 2013). Intensity Theory focused on pain not as a unique sensory experience but rather as an experience that results from a stronger stimulus than usual (Dallenbach, 1939). Support for Intensity Theory came from experiments showing that repeated sub-threshold tactile and electrical stimulation produced pain in patients with syphilis who had deteriorating dorsal columns (Dallenbach, 1939). In contrast, Specificity Theory posits that each somatosensory modality, including pain, has a specific receptor; the associated primary afferent is sensitive to one specific stimulus (Dubner, Sessle, & Storey, 1978). Noxious stimuli from the environment activate pain receptors (i.e., nociceptors) which project to higher pain centres in the brain through a pain fibre, resulting in the perception of pain. Support for this theory came from,

among others, Burgess & Perl (1967) and Bessou & Perl (1969), who discovered myelinated and unmyelinated primary afferent fibers that only responded to noxious stimuli. In contrast to Intensity Theory, Specificity theory led to the notion of labelled lines that carry specifically pain related information to the brain.

Around the same time that Specificity Theory was proposed, a competing theory called Pattern Theory was gaining traction. Pattern Theory posits that any sensation – be it pain, vision, or mechanoreception – arises from a specific pattern of neural firing; the spatial and temporal firing patterns of peripheral nerves dictate the stimulus type and intensity (Lele, Sinclair, & Weddell, 1954). Backing for this theory came from work which showed that pain was perceived from intense stimulation of encapsulated or non-encapsulated nerve fibres (Sinclair, 1955).

Eventually, the seemingly opposing Specificity and Pattern Theories were brought together with the Gate Control Theory that revolutionized pain research (Melzack & Wall, 1965). This theory suggested that afferent fibres carry noxious stimuli from their respective nociceptors and synapse in the spinal dorsal horn. If the intensity of the noxious stimulus was strong enough, it would "open the gate" and give the sensation of pain. This gating mechanism was also controlled by large fibres, which closed the gate, and small fibres, which opened the gate. Uniquely, Gate Control Theory proposed that the gate could be opened or closed by supraspinal structures through descending projections, providing a higher-order modulatory apparatus for pain perception.

While these theories effectively described observations regarding nociception, none accounted for the full complexity of this system. For example, these theories did not address mechanisms of persistent or chronic pain (CP), instead focusing on cutaneous stimulation, likely because it was assumed that the nervous system was non-adaptive, or hard-wired (Moayedi &

Davis, 2013). Although the mechanisms of pain chronification are still being intensely studied, it is now understood that plasticity in both the central and peripheral nervous systems is common following repeated nociceptive stimulation in healthy individuals (Davis & Moayedi, 2013). Nonetheless, the rise of Gate Control Theory started to change the pain research landscape from one that defined pain as a unidimensional construct to one that defined pain as multidimensional and variable to individual and environmental differences (Seymour, 2019).

1.1.3. Current Frameworks of Pain

Today, pain is seen as having multiple facets, involving sensory-discriminatory (e.g., duration, intensity, and location), affective-motivational (e.g., unpleasant emotions such as fear), and cognitive-evaluative (e.g., context, attention, and biological significance) components that comprise an individual's perception of pain (Melzack & Casey, 1967; Seymour, 2019). Using this framework, pain may act as a motivational signal to the organism to change behaviour that maintains homeostasis (Fields, 2018). The response to pain depends on differing motivational values of alternative actions, such as short-term escape-oriented behaviour to evade pain versus long-term avoidance behaviours (Seymour, 2019). Pain, then, is not only a signal for passively recording nociceptive inputs, but also a predictive mechanism that allow organisms to maximize rewards and minimize harms. In a similar vein, pain can be seen as a learning signal whereby organisms can change future behaviour to avoid noxious stimuli (Fields, 2018).

Overall, pain perception is a combination of bottom-up (e.g., stimulus intensity and duration) and top-down (e.g., expectations, attention) signals, but this integration of the pain response is a relatively less researched topic. This is mainly because the role of the brain in pain perception is unclear; the brain's main function is to give meaning to sensory objects and to store information. These 'top-down' factors are less clearly understood in pain research. In the current

thesis, pain was explored as the integration between bottom-up and top-down signals and how pain signaling can go awry in a population where pain is chronic and loses its reward value.

1.2. Chronic Pain

1.2.1. Overview

While acute pain is necessary for survival, encouraging humans to avoid tissue damage and seek healing, CP has no such beneficial value. Instead, CP produces significant economic, social, and clinical burdens to individuals and society (Katz, Rosenbloom, & Fashler, 2015). Chronic 'primary' pain is defined by IASP as pain in one or more regions that persists for longer than three months and is accompanied by significant functional disability and distress, while chronic 'secondary' pain is associated with another disease that is the underlying cause. Regardless of whether CP is primary or secondary, it is a complex phenomenon involving sensory systems and threat neurocircuitry relating to emotional and cognitive components, including the nucleus accumbens (NAc), medial prefrontal cortex (mPFC), and amygdala (Elman & Borsook, 2018; Hashmi et al., 2013).

1.2.2. The Costs of Chronic Pain

In Canada, one in every five people suffer from this debilitating, unpredictable disorder (Shupler, Kramer, Cragg, Jutzeler, & Whitehurst, 2019). Chronic back pain (CBP) is particularly challenging, as it pervades the entire nervous system and especially the brain with a distinct pathology (Hashmi et al., 2013). Economically, CP costs the Canadian government $60 billion per year in direct costs related to health care and indirect costs related to lost productivity (Phillips, 2014). Socially, CP restricts patients' leisure activities and social contacts. Around half of patients with CP report an inability to attend social or family events due to their condition

(Moulin, Clark, Speechley, & Morley-Forster, 2002). Clinically, CBP patients often do not respond to analgesic therapy (Simon, 2012): many people with CBP report not only intense treatment refractory back pain (i.e., pain following treatment cessation), but also complex symptoms such as pain comorbidities, psychological distress, and skewed treatment expectations generated from a long history of failed treatments (Simon, 2012). Often, repeated treatment failures leave CBP patients with co-morbid affective conditions (Simon, 2012). Indeed, a population survey involving 85,088 participants found that mood and anxiety disorders were more common among those with chronic back or neck pain compared to those without (Demyttenaere et al., 2007). Comorbid disorders in CP patients frequently result in a positive feedback loop: a decline in physical capacity and mental health observed in CP patients contributes to their impaired social integration, which leads to further deterioration in their health and further social isolation (Dueñas, Ojeda, Salazar, Mico, & Failde, 2016).

1.2.3. The Brain and Chronic Pain

Since the ineffectiveness of mainstream pharmacological pain treatments for CBP is widespread, it is imperative to re-evaluate the way that pain is represented and managed. Patients referred to pain clinics frequently present with complex pain symptoms, pain co-morbidities, and psychological manifestations that require lengthy assessments and specialized clinical experience for proper diagnosis and treatment. Because of this complexity, treatment response to analgesics in CBP patients may be pre-determined by patient-specific factors related to their brain structure and psychology. One of the promising fields of research in this realm involves understanding treatment expectations in CBP. It has been reported that one of the strongest contributors to treatment response in CP is expectation (Enck, Bingel, Schedlowski, & Rief, 2013; Vase et al.,

2015). Thus, part of this thesis aims to determine the role of expectation in pain perception, and how specific neural regions activate to different expectation effects.

Many current empirical questions about CP lie in the purview of neuroscience: for example, what neural networks underlie CP, and can it be predicted based on observable brain characteristics? Answering these questions is difficult because, as established previously, pain is multifaceted, with both bottom-up factors such as noxious stimulus intensity and top-down influences such as expectation effects influencing pain perception (Elman & Borsook, 2018; LeDoux & Daw, 2018). Current evidence suggests that top-down factors modulate nociceptive bottom-up input and alter the experience of pain through a connected network of neural regions (Fields, 2018). Among functional systems, the reward circuitry (including regions within the striatum) has emerged as the most affected in people with chronic pain. Striatal regions are important for the motivational-affective dimension of CP and act as a centre for dopaminergic inputs (DosSantos, Moura, & DaSilva, 2017); it is this system that is currently an important target for uncovering chronic pain aetiology. One substructure of the ventral striatum, the NAc, is of particular interest in this thesis, due to its role in mediating motivation-oriented behaviour (Heimer, Zahm, Churchill, Kalivas, & Wohltmann, 1991).

1.3. Bottom-Up and Top-Down Factors Affect Pain Perception

1.3.1. Propagation of the Pain Response

Noxious stimuli are sensed by nociceptors and conducted primarily through two types of afferent nociceptive fibres, A-delta and C fibres (Djouhri, 2016). While A-delta fibres are myelinated and have a large diameter, C fibres are not myelinated and are smaller. Thus, A-delta fibres conduct pain at faster rates than C fibres and tend to respond to superficial, sharp, or fast thermal inputs, while C fibres typically respond to deep, dull, or slow thermal stimuli (MacIver

& Tanelian, 1993). Both A-delta and C fibres synapse to lamina I within the spinal dorsal horn before being relayed by second-order neurons to supraspinal targets (Rexed, 1952).

From the spinal dorsal horn, second-order neurons arrange into three different tracts – the spinothalamic, spinoreticular, and spinomesencephalic tracts – that decussate to the contralateral side of the spinal cord to carry the noxious information to supraspinal regions (Patestas & Gartner, 2016). The spinothalamic tract is itself divided into two main paths, the lateral and anterior tracts, that project to distinct areas in the thalamus to facilitate sensory-discriminative aspects of pain primarily through A-delta afferent fibres (Willis & Westlund, 1997). While the lateral tract arises from lamina I, the anterior tract arises from laminae IV and V (Apkarian & Hodge, 1989); both chiefly have roles in pain perception (Patestas & Gartner, 2016). The indirect, multi-synaptic, and phylogenetically older spinoreticular tract begins with C fibres and synapses in the dorsal horn to ascend through the ventrolateral region of the cord before synapsing to the medulla (Patestas & Gartner, 2016). It is thought that this pathway carries dull and slow pain and is involved in the motivational and emotional characteristics of pain (Almeida, Roizenblatt, & Tufik, 2004; Panneton, Gan, & Ariel, 2015). Finally, the afferent fibres in the spinomesencephalic tract travel through the spinoannular bundle and terminate predominantly in the periaqueductal grey (PAG) and raphe nuclei (Almeida et al., 2004); this is thought to be a pain inhibiting pathway (Yezierski, 1990). These different anatomical projections demonstrate the complexity of the different pain networks that are responsible for pain perception.

1.3.2. Bottom-Up Signals are Perceived Differently Based on Stimuli Characteristics

Distinctions between A-delta and C fibres, as well as their respective tracts, allow for different characteristics and types of pain to be perceived (Madsen, Johnsen, Fuglsang-Frederiksen, Jensen, & Finnerup, 2012). This distinction provides an interesting area for research

study involving different stimuli that target one group of nociceptors over another. Human experiments using painful stimuli have mainly focused on static stimuli: in the case of heat pain, this means that the temperature plateaus after reaching a target temperature. Dynamic stimuli, by contrast, involve unpredictable temperature changes. Static and dynamic thermal stimuli are perceived differently (Hashmi & Davis, 2008, 2009): the absence of changes in temperature is perceived differently from situations where the stimulus intensity is unpredictably increasing. Additionally, in real-world situations, noxious stimuli are rarely static. Hence, dynamic stimuli represent a more ecologically valid pain stimulus. Since pain pathways are organized to detect physical threats and predict upcoming threats (Yam et al., 2018), static stimuli result in pain adaptation because top-down systems allocate resources primarily to detecting changes. For example, Hashmi & Davis (2008) found that for the first heat stimulus, sharp, stinging, and cutting sensations attenuated in response to static stimuli but intensified in response to dynamic stimuli; during subsequent stimuli, responses for sharp sensations habituated relatively more than burning sensations. Further research also showed sex differences in the time course of pain (Hashmi & Davis, 2009). These findings suggest that for static stimuli, burning sensations, a quality associated with polymodal C-fibers, are more involved in encoding pain responses to static stimuli. In comparison, dynamic stimuli show less adaptation and habituation in sharp stinging sensations relative to static stimuli. Since sharp sensations are associated with A-delta receptor activity, these findings indicate that pain responses to dynamic stimuli are mediated by a combination of A-delta and C-fiber activity.

A study by Beissner et al. (2010) found that verbal descriptions of pain sensations were able to accurately distinguish between A-delta and C fibre mediated pain, with the descriptors ‘pricking’ being associated with A-delta fibres, and ‘pressing’ and ‘dull’ being associated with C

fibres. This, and some animal studies (Yeomans, Pirec, & Proudfit, 1996) have suggested that fast rising stimuli exclusively activate A-delta receptors and produce sharp/pricking sensations. Finally, firing rates of A-delta type 2 and C fibers initially increase dramatically at the onset of static stimulation before gradually attenuating to a level comparable to that of the background activity of those neurons (L. Li, Mi, Zhang, Wang, & Wu, 2018). Pain in static stimuli, therefore, can be taken as a combination of bottom-up nociceptive firing and top-down modulation (Andrew & Greenspan, 1999). On the other hand, with dynamic stimuli, detection plays a key role, prompting nociceptive circuits to stay vigilant (Dostrovsky & Craig, 1996).

1.3.3. Top-Down Control of Pain Signals

Painful external stimuli ascend to the neocortex via pain pathways, but these bottom-up signals undergo modulations at several levels: for example, these nociceptive inputs are amplified or dampened by top-down factors such as prior expectations and attention (LeDoux & Daw, 2018; Lim et al., 2020). When prior expectations do not match bottom-up nociceptive signals, the brain will either learn from the error and update its expectations or top-down factors will bias pain perception and the sensory input will be altered.

So far, it is known that expectations generated from prior learning using Pavlovian cues or associative learning are known to alter perceived pain intensity and are mediated, in part, by specific neural circuitry and psychological variables (Atlas, Bolger, Lindquist, & Wager, 2010; Kong et al., 2013; Lim et al., 2020; Shih et al., 2019). Atlas et al. (2010) used auditory cues to elicit expectations for barely painful or highly painful thermal stimulation. These cues influenced heat-evoked responses in most canonical pain processing regions and a subset of these regions, including the anterior cingulate cortex (ACC), anterior insula, and thalamus, were found to mediate cue effects on pain. Their results suggest that activity in pain processing regions reflects

a combination of nociceptive input and top-down information related to expectations. Kong et al. (2013) found that subjective pain ratings were significantly altered by visual cues that simply said ‘high’ or ‘low’ before presentation of heat stimuli. These cues were conditioned through matched heat stimuli and subsequently, the pairing was changed so that high cues were paired with low intensity stimuli; this significantly reduced evoked pain intensity. The findings demonstrated that cued expectations could alter pain perception. Frontoparietal and emotional regulation (e.g., rostral anterior cingulate cortex; rACC) regions were involved in cue modulation; resting state functional connectivity (rsFC) between the frontoparietal network and the mPFC/rACC was positively correlated with cueing effects on pain perception. This suggests that frontal networks are important in the generation of expectation effects.

Shih et al. (2019) focused on the difference between positive and negative expectations using fMRI in a stimulus expectancy paradigm, finding that positive and negative expectations altered pain intensity and engaged the right anterior insular cortex (aIC) and right rACC, respectively. Participants’ certainty about expectations predicted the extent of pain modulation such that positive expectations involved connectivity between aIC and hippocampus, a region understood to regulate anxiety, while negative expectations involved connectivity between the rACC and lateral orbitofrontal cortex, a region postulated to reflect outcome value and certainty.

Finally, Lim et al. (2020) used a higher-order schema model instead of simple associative learning (via Pavlovian conditioning) or explicit conditioning used in the aforementioned studies. Instead, participants were taught a linear association where visual cues matched the heat stimuli without explicit instruction. Afterward, prediction error was introduced such that linearity was reduced gradually, and participants partially updated their evaluations of pain in relation to the stepped increases in prediction errors. The authors found that cognitive, striatal, and sensory

regions graded their responses to changes in predicted threat despite prediction errors. Psychologically, individuals with higher catastrophic thinking and lower mindfulness on self-reported scales were significantly more reliant on the schema than on the sensory evidence from the pain stimulus, which mapped to variability in responses of the striatum and ventromedial prefrontal cortex (vmPFC).

In these prior studies, expectations were tested by pairing positive or negative expectancy cues with stimuli that are static. However, in real-world situations, noxious stimulus intensity often fluctuates and can escalate over time and requires adaptive response generation. As well, dynamic stimuli putatively activate nociceptive signalling through A-delta receptors. These nociceptors are myelinated and have higher conduction velocities and hence respond to fast onset noxious events and encode sharp pain sensations. Hence, dynamic stimuli, where heat stimuli are constantly changing, represent a novel stimulus type for observing how expectations influence important pain-processing regions like the NAc. The NAc engages in events that involve dynamic alterations in the relation between probability of reward and decisions (Nachev et al., 2015). Thus, the role of the NAc in static vs dynamic expectations has been suggested but has not been thoroughly investigated. One approach is to compare NAc response patterns between pain evoking stimuli that have static or dynamic intensities; incorporating these two types of noxious stimuli may provide valuable information due to their underlying differences in motivational salience and fibre transmission mechanisms.

As well, while these studies reliably show that many different brain regions control pain perception to incorporate both bottom-up and top-down factors, they analyze whole brain differences and exclude analyses of relevant pain regions like the NAc. Therefore, this thesis

focuses on whether expectations alter pain perception and NAc activation in static and dynamic noxious heat differentially.

1.4. The Nucleus Accumbens

1.4.1. Overview

The nucleus accumbens is a region within the ventral striatum generally referred to as the primary reward centre due to its role in motivating hedonic behaviour (Ikemoto & Panksepp, 1999). The NAc is a critical structure involved in motivational, emotional, and reward processes, and in mediating the effects of certain drugs (Salgado & Kaplitt, 2015). It is also thought to mediate the limbic-motor interface and has been implicated in a wide range of neuropsychiatric disorders, including depression, anxiety, drug abuse, and chronic pain (Makary et al., 2020; Salgado & Kaplitt, 2015). It is becoming clear that the NAc is not only important in rewarding events, but also in threatening and aversive (Harris & Peng, 2020), motivationally salient (Kim, Nanavaty, Ahmed, Mathur, & Anderson, 2021) and surprising (Shulman et al., 2009) events. Clearly, the NAc is multi-dimensional: it helps determine the motivational salience of positive and negative events as well as the efficiency and vigor of behaviour toward intended goals (Floresco, 2015; Harris & Peng, 2020).

Accumbal activity is greater in response to reward-predictive cues compared to neutral cues in non-primate animals; similarly, negative valence associated with cues learned from aversive stimuli also activates the NAc (M. H. Ray, Moaddab, & McDannald, 2022). The NAc is necessary for exploratory and withdrawal decisions (Piantadosi, Yeates, & Floresco, 2018) that involve discriminating the validity of threats. However, there is ambiguity around the specific noxious sensory events that activate the NAc. There are few studies that have directly investigated modulations in NAc responses to noxious stimuli presented under low or high threat

valence. In addition, the NAc plays a role in detecting uncertainty and learning from prediction error (S. S. Li & McNally, 2015; M. H. Ray et al., 2022), but little is known whether false cues of threat or safety can be encoded by the NAc. The NAc broadcasts teaching signals for learning that lead to behaviours that maximize reward and minimize pain through multi-functional signals shared with a variety of striatal and cortical regions. The motivation to avoid pain is among its key functions despite its known role in encoding reward. Nevertheless, few studies have observed NAc responses to noxious events under different expectation conditions.

Predicting reward and threat is essential for survival. Animals can learn about events with positive and negative valence events and can build top-down expectations about their occurrence. Due to the NAc's involvement in learning and determining the motivational salience of stimuli, especially in unpredictable situations (Berns, McClure, Pagnoni, & Montague, 2001), the NAc was specifically targeted in this thesis. Reasonably, the motivation for seeking reward is on par with the motivation for avoiding pain, and thus the NAc should play a crucial role in both hedonic and threat-related processes. Indeed, the NAc activates to violations in expectations of reward and responds to noxious stimuli (Fields, 2018; Spicer et al., 2007). Interestingly, the NAc seems to activate prior to canonical pain areas, and both pain- and reward-associated cues produce strong activations in the NAc (Fields, 2018). Additionally, the accumbens is a structurally and functionally heterogenous region comprised of the core and shell; these subregions have dissociable roles and functional connectivity profiles (M. N. Baliki et al., 2013; S. H. Xia et al., 2020).

1.4.2. Anatomical and Functional Differences Between the Shell and Core

In humans, the NAc is found anterior to the posterior border of the anterior commissure and lies parallel to the midline (Salgado & Kaplitt, 2015). The NAc can be further divided into an outer shell that surrounds a central core.

Differences between the core and shell reside on the molecular level: while the core tends to harbour receptors for calbindin, enkephalin, and $GABA_A$, the shell tends to harbour receptors for substance P, calretinin, serotonin, and dopamine (Berlanga et al., 2003; Salgado & Kaplitt, 2015). Projections from the core and shell are also different: core connectivity eventually leads to premotor and supplemental motor areas of the cortex; shell connectivity leads to prefrontal cortical areas, the extended amygdala, and the lateral hypothalamus (Salgado & Kaplitt, 2015). As well, independent from shell-core distinctions, there is also a rostrocaudal gradient of D1 and D2 receptors and a lateral-to-medial gradient of D2 receptors in rats (Bardo & Hammer Jr, 1991).

These two substructures of the NAc are thought to have dissociable roles in signaling rewarding versus aversive events as well as different functional connectivity profiles (M. N. Baliki et al., 2013; S. H. Xia et al., 2020; X. Xia et al., 2017). Functionally, the shell is thought to play a role in suppressing non-rewarding stimuli through value-based decision making (S. H. Xia et al., 2020; X. Xia et al., 2017). In contrast, the core plays a role in selectively instigating an approach toward the incentive stimulus associated with the best available reward (S. H. Xia et al., 2020; X. Xia et al., 2017).

A large body of experimental work suggests that dopamine neurons, especially the NAc core, encode both positive and negative prediction errors (cue-stimuli violations) (Badrinarayan et al., 2012; Hart, Rutledge, Glimcher, & Phillips, 2014; M. H. Ray et al., 2022). In contrast, the shell encodes the incentive salience of stimuli (Saddoris, Cacciapaglia, Wightman, & Carelli,

2015). Thus, the shell and core should have dissociable roles in responding to cue-stimuli violations in humans, although this has never been tested before using predicted threat and noxious event paradigms. Moreover, observing NAc core and shell responses separately may help in disentangling effects of expectations on shell and core responsiveness that have hitherto remained elusive.

1.4.3. The Nucleus Accumbens and Chronic Pain

While distinct functional connections between the NAc substructures are apparent, scant research has directly compared core and shell resting state connectivity and network profiles between HC and CBP patients. Previous reports suggest that NAc connectivity with the medial prefrontal cortex (mPFC) extending into the dorsal ACC measured in the subacute back pain (SBP) phase, predicts the transition to CBP (M. N. Baliki et al., 2012). The mPFC/ACC is important for pain monitoring and responds to perturbations in chronic, but not subacute, back pain. The mPFC/ACC is a key component of the default mode network (DMN) and is important for goal directed behaviors and social cognition. Subsequently, it was shown that NAc functional connectivity with a more dorsal part of the DMN (the dorsal mPFC) was higher in people with SBP who later developed chronic pain. Recently, Makary and colleagues (2020) found decreased functional connectivity between the left shell and the left thalamus, right caudate, and rostral ACC in persistent CBP patients compared to HC. A systematic comparison between groups for elucidating variability in core and shell functional connectivity profiles within canonical resting state networks can direct us to the function of NAc in chronic pain aetiology. Because of these functional differences in the core and shell, part of this thesis sought to test for differences in NAc subregion functional connectivity.

Converging evidence from animal and human research has implicated the reward circuitry, especially the NAc, in the aetiology of chronic pain. Evidence points to the NAc as a critical area in the evolution from acute to CP; its activity and connectivity with medial prefrontal cortex and size has even been posited as 'biomarkers' for CP (M. N. Baliki et al., 2012; Makary et al., 2020).

Additionally, given that the NAc is known for its role in encoding reward values and prediction error, it should come as no surprise that the NAc is greatly affected by states of stress (Castro & Bruchas, 2019). In animals, dopamine levels increase in response to stress (Kalivas & Duffy, 1995), and repeated stress alters signaling to the NAc and leads to depressive symptomology (Francis & Lobo, 2017). In addition, the motivational salience of aversive events is perceived as higher in anxious individuals (Charpentier, Aylward, Roiser, & Robinson, 2017). Recent reports demonstrate that the NAc core plays a role in scaling fear to the degree of threat and thus allows discrimination between threat and safety (Madelyn H Ray, Russ, Walker, & McDannald, 2020). Thus, the NAc may be altered over the course of CP, a condition associated with significant stress and co-morbid disorders like depression.

Despite this research, direct comparisons of core and shell resting state profiles between HC and longer-term CBP groups remain inconclusive. As well, it is unknown whether these differences can predict clinical pain outcomes or be used to distinguish between groups.

1.5. Objectives and Hypotheses

While static stimuli have been previously tested in heat expectation paradigms, the effect of dynamic stimuli on pain perception remains unknown, as well as the mechanisms underlying pain perception during different expectation effects in the NAc and its subregions. Additionally, because CBP patients have a long history of expected treatment failure, and previous research

has implicated the NAc in mediating expectation effects and in the aetiology of CBP, another aim was to systematically characterize differences in NAc core and shell activity between healthy individuals and CBP patients. Therefore, in this thesis, the objectives were to:

1) Understand how participants respond behaviourally (via pain ratings) to static and dynamic stimuli as well as to expectation effects.
2) Determine whether differences in stimuli characteristics and expectation effects map onto whole and subregion (shell and core) NAc activation.
3) Analyze differences in resting state connectivity of the shell and core within and between healthy individuals and those with chronic back pain, map these connections onto resting-state networks, and find reproducible connections that can distinguish between these two groups.

Therefore, the first part of this thesis sought to elucidate the mechanisms underlying pain perception during different expectation effects and stimulus characteristics in the NAc and its subregions. A novel expectation paradigm was used in which cued threats signaled unknown, low, or high impending thermal pain. Actual pain was either in line with expectations (the matched conditions) or opposite of expectations (the mismatched conditions) to introduce prediction error. As well, stimuli were either static or dynamic. Nucleus accumebns activation during presentation of expectation cues, during noxious stimulation, and during the evaluation of pain were analyzed. Behaviourally, pain ratings during different combinations of stimuli characteristics and expectation effects were analyzed. It was hypothesized that expectation effects (difference in pain ratings between matched and mismatched conditions) would be greater in static stimuli relative to dynamic stimuli due to greater pain adaptation in static stimuli. As well, it was hypothesized that positive expectations would significantly lower pain ratings and

negative expectations would significantly increase pain ratings. Furthermore, since the NAc core is important in encoding threat and prediction error, it was hypothesized that the blood oxygenation level dependent (BOLD) signal in the NAc would be greater during heat in epochs with cue-stimuli violations relative to matched cue-stimuli associations.

During the second part of this thesis, resting state networks (RSNs) associated with the two NAc substructures in CBP patients and HC, as well as their clinical significance for CBP, were assessed. First, the resting state functional connectivity (rsFC) of the core and shell to other neural regions was assessed separately in HC and in CBP patients (core > shell and shell > core). Based on previous literature showing differences in core and shell connectivity, it was hypothesized that the core would be more connected to salience and motor regions, and the shell would be more connected to default mode and prefrontal regions. Then, differences in core and shell connectivity were compared between HC and CBP patients (CBP > HC and CBP < HC). It was hypothesized that NAc core and shell rsFC would be higher to prefrontal and default mode regions in CBP patients relative to HC, while HC would have higher core and shell connectivity to salience and subcortical regions. The significant within- and between-group connections were mapped to one of five canonical RSNs: default mode, salience, language/memory, subcortical, or attention/executive networks for interpretation (Hashmi et al., 2017; Saghayi et al., 2020). Finally, the correlation between the identified connections in the CBP > HC and CBP < HC contrasts and self-reported clinical pain of CBP patients were assessed. These connections were also assessed for reproducibility in a separate cohort of CBP patients and HC. It was hypothesized that the significant CBP > HC and CBP < HC connections would be correlated with measures of chronic pain intensity.

CHAPTER 2. Materials and Methods

2.1. Participants

These studies were approved by Nova Scotia Health Research Ethics Board. Healthy and CBP participants were recruited via advertisements posted in the community around Dalhousie University and Victoria General Hospital in Halifax. Chronic back pain patients were also recruited from the Pain Management Unit of the Victoria General Hospital and other clinical centres in the community. Both HC and CBP patients were required to be right-handed, as certain cognitive processes, such as sensation, are represented differently in the brains of adextrals. Additionally, to include left-handed participants, the sample size would need to double. Since handedness was not a specific topic for investigation in this study, only right-handed participants were included. Other criteria included being between the ages of 18–75 years, and comfortable with reading, writing, and taking instructions in English. Participants were excluded if they had medical conditions that would interfere with the study (e.g., respiratory or cardiac conditions), contraindications to MRI scanning (e.g., claustrophobia, metal implants, or dental braces), or visual impairment that could not be corrected with eyewear or contact lenses. Healthy participants were excluded if they had ongoing acute pain, CP, nerve compression resulting in sensory loss, or if they were taking pain medications. Chronic back pain patients were required to have low back pain for six or more months and a score of at least 4/10 on the Brief Pain Inventory (Cleeland, 1989) two weeks prior to enrolment.

For the first part of this thesis, 35 healthy adults were recruited. Five of these participants completed all testing outside the MRI scanner. The remaining participants (n = 30) completed resting-state scans and task scans (the experimental protocols) inside the scanner. The protocols inside the scanner included one resting-state scan and four task scans. The 30 resting-state scans

collected from the first part of the thesis were used in the second part as the HC validation dataset (only the task scans were of interest and analyzed for the first part of this thesis).

For the second part of this thesis, based on the inclusion and exclusion criteria, 44 HC and 72 CBP patients were recruited as part of a larger study directed at understanding biopsychosocial and neurological factors associated with treatment failure in CBP (clinicalTrials.gov: RCT #NCT02991625). From this initial pool, some subjects were removed due to withdrawal (CBP: 2, HC: 1), medical considerations (HC: 2), undisclosed contraindications to MRI (CBP: 1), and difficulty following instructions (CBP: 1; see Figure 2. 1. for details). Additionally, neuroimaging data could not be collected from 11 CBP patients due to equipment failure. Therefore, behavioural and neuroimaging data from 41 HC (22 females, age range 20–56 years old) and 57 CBP patients (39 females, age range 18–71 years) were used in analysis. Additionally, a validation dataset was used with a separate cohort of HC and CBP groups. These included 30 HC (18 females, age = 27.6 years, age range 18–61) that participated in the first experiment (see preceding paragraph) and an additional 18 out of sample CBP patients (15 females, age range 23–56) patients. However, there was no overlap of data used, since the first study analyzed task-based fMRI data, while the second analyzed resting-state

fMRI data.

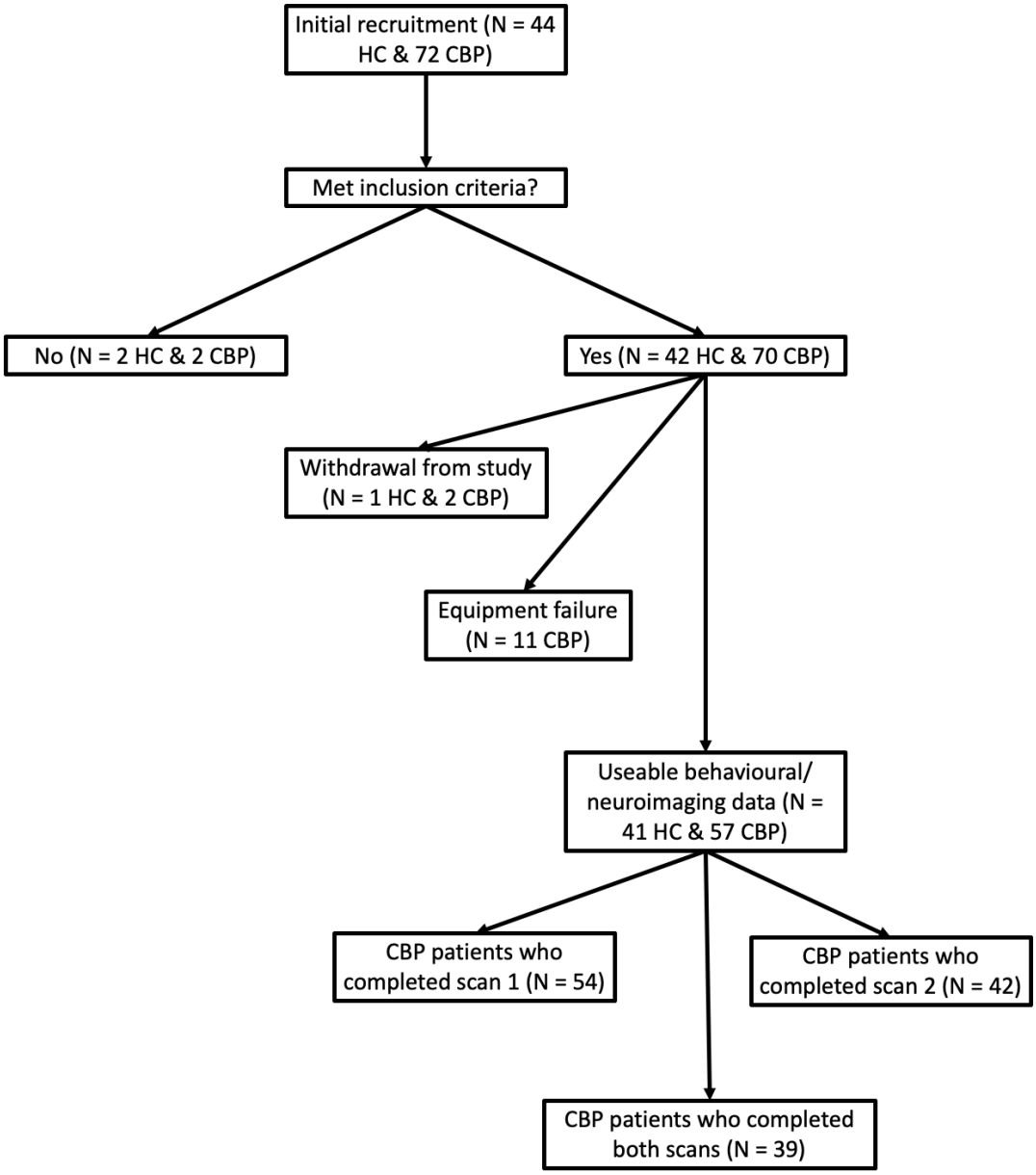

Figure 2. 1. Flow chart of the data used in the initial dataset.

2.2. Experimental Design

For project one, noxious heat was applied to the skin on participants' left lower leg using an MRI-compatible thermal probe (QST.Lab Thermal Contact Stimulator II; QST; BIOMED ID: 47297; Strasbourg, France) which contains safeguards to prevent injuries. Before the MRI scan,

the QST was first used to test heat pain threshold, tolerance, and sensitivity using the method of limits. Briefly, the temperature was increased from a baseline of 35°C at a rate of 1°C/s and the participant pressed a button to terminate the stimulus as soon as they detected pain (to measure pain threshold) or as soon as the evoked pain was intolerable (to measure pain tolerance).

Next, participants were instructed on how to use the Numerical Rating Scale (NRS; 0-100) with visual anchors on the left (0 = no pain) and right (100 = worst pain imaginable) sides of the screen. During the rating period, participants were able to move the cursor, which was initially placed at 50, to select the score representing their pain by pressing two buttons on an MRI-compatible response device (Lumina LSC-400 controller, Cedrus) in their right hand. All pain ratings and reaction times were acquired using Presentation software.

As per previous protocols (Lim et al., 2020), the heat stimuli started at a baseline of 35°C. A general outline of events for each epoch is depicted in Figure 2. 2. A. Participants were first presented with a cue that varied depending on the stage of the experimental paradigm. First, participants were presented with an unknown cue ("The incoming heat is at x% intensity") followed by a heat stimulation and then a rating period. Stimuli peaked at either 45°C or 47°C, and stimulus characteristics were either static or dynamic. Temperatures were the same for every participant and not based on individual thresholds to standardize the heat stimuli across all participants; these standard temperatures were also in line with pervious protocols (Lim et al., 2020). The different combinations of cues, temperatures, and stimuli characteristics are represented in Figure 2. 2. B.

The flow of task scans is depicted in Figure 2. 2. C. After the first task scan, which consisted of 12 epochs with unknown cues, the second task scan consisted of 12 'matched' epochs in which cues were either low (15%) or high (90%) and the temperatures were 45°C and

47°C, respectively. Therefore, participants were trained to associate low threat cues with low temperatures, and high threat cues with high temperatures across static and dynamic trials. For the final two task scans of 16 epochs each, mismatched conditions were introduced such that low threat cues were paired with 47°C (positive expectation) and high threat cues were paired with 45°C (negative expectation). This introduced prediction error, whereby participants received a heat stimulus that was not in line with the anticipation of heat intensity based on information from the cue. While most epochs in each mismatch scan consisted of either positive or negative expectations, five and six epochs in mismatch scans one and two, respectively, were matched to preserve the association learned in the matched condition. Additionally, cues were varied during the task scans such that low and high cues were pulled from a range (1-20% and 80-100%, respectively) to reduce learning. All epochs were delivered in a pseudorandom sequence, and the thermal probe was moved to a different skin patch after every scan to reduce sensitization or habituation effects. Overall, the cue was presented for 4.75 s, the heat for 8.075 s, and the rating scale for 5.7 s. After the cue presentation ended and before the heat application started, there was an interstimulus interval of 4 s. As well, after heat application ended and before the rating period started, there was an interstimulus interval of 5 s. Following each epoch, a variable rest period of 1.9 s to 7.6 s ensued before the cue of the next epoch was presented.

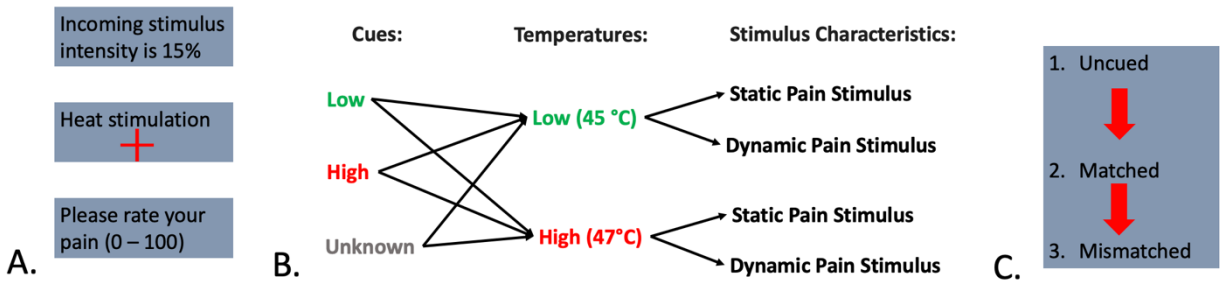

Figure 2. 2. Illustration of the experimental paradigm. **A.** During each epoch, predictive cues were presented before a heat stimulus; the heat stimulus was followed by a prompt for pain rating on a 0–100 visual analog scale. The cued

threat changed depending on the condition. **B.** Three cue types, two temperatures, and two stimulus characteristics were used in the design. **C.** The flow of scans. First, subjects underwent the uncued scan, where the presented cue was 'x', the temperature was either 45°C or 47°C, and the stimulus was either static or dynamic. During the matched scan, the cues (15% or 90%) predicted the heat stimulus temperature. During mismatched scans, predictive cues were divided into two groups (1-20%, 80-100%). The stimulation was usually opposite of the cue presented (e.g., 10% cue paired with 47°C), although some epochs were matched to reduce the rate of learning.

Both static and dynamic stimuli were designed to last eight seconds from start to finish and have similar amounts of time at peak stimulus temperature. At the high temperature, the static stimulus rose from 35°C to 47°C at a steady 5°C/s and returned to baseline at the same rate. Therefore, 2.4 s were allotted for ramp up and down time, and the temperature was held at 47°C in-between the ramp up and down time (3.3 s). At the low temperature, the ramp rate remained at 5°C/s, giving 2 s each for ramp up and down time, and 4.07 s at 45°C.

For dynamic stimuli, the ramp rate was 25°C/s for both the 45 and 47°C stimuli. During the 45°C stimulus, the temperature rose from 35°C to 43°C and stayed there for 1 s; rose to 44°C and remained there for 2.5 s; then finally reached 45°C and remained there for 4.05 s before returning to baseline. During the 47°C stimuli, the temperature rose to 45°C and remained there for 1.1s; increased to 46°C and remained there for 3.02s; then finally increased to 47°C and remained there for 3.15s before returning to baseline. As well, static and dynamic stimuli were analyzed within-subjects; all participants experienced both types of stimuli.

2.3. Questionnaires

In both studies, participants answered a series of psychological questionnaires via REDCap (http://www.project-redcap.org) using an iPad; data were stored electronically. For the first study, participants were asked for their responses on the Beck Depression Inventory-II (BDI) (Beck, Steer, Ball, & Ranieri, 1996), the State-Trait Anxiety Inventory (STAI)

(Spielberger, 2010), and the Five-facet Mindfulness Questionnaire (FFMQ) (Baer, Smith, Hopkins, Krietemeyer, & Toney, 2006). For the second part of the study, both HC and CBP participants answered the Pain Catastrophizing Scale (PCS) (Sullivan, 1995) and BDI. CBP patients also completed the Neuropathic Pain Scale (NPS) (Galer & Jensen, 1997), the McGill Pain Questionnaire short form (MPQ) (Melzack, 1987), and the Brief Pain Inventory (BPI) (Cleeland, 1989). Participants also provided information on medications they were currently taking to manage their pain, which was quantified using the Medication Quantification Scale (MQS) (Harden et al., 2005).

2.4. fMRI Data Acquisition and Preprocessing

All images were collected with a 3.0 T MRI scanner (Discovery MR750; General Electric Medical Systems, Waukesha, WI, USA) with a 32-channel head coil (MR Instruments, Inc., Minneapolis, MN, USA) at the Biomedical Translational Imaging Centre (BIOTIC) at Veterans' Memorial Building of the Queen Elizabeth II Health Sciences Centre in Halifax, NS, Canada. To minimize movement, participants' heads were fitted with foam padding. Participants were reminded to keep their head still before each scan took place, and ear plugs were provided to reduce noise levels.

We gathered T1-weighted anatomical images (GE sequence IR-FSPGR: field of view=224×224×184 mm; in-plane resolution=1×1×1 mm; TR/TE=4.4/1.908 ms; flip angle=9°) from both HC and CBP patients. Blood oxygenation level dependent signal sequences for fMRI were acquired using a multi-band EPI sequence: field of view=216×216×153 mm; in-plane resolution=3×3×3 mm; TR/TE=950/30 ms, SENSE factor of 2, acceleration factor of 3. Multibanding, where multiple brain slices are excited and acquired concurrently, at the moderate acceleration factor (3) used in this thesis can gather more information during task-based fMRI.

This type of data acquisition is relatively new and has been suggested to improve data quality significantly (Chen, Adleman, Saad, Leibenluft, & Cox, 2014). However, higher sampling rates (>3) significantly drops the signal to noise ratio (Daranyi, Hermann, Homolya, Vidnyanszky, & Nagy, 2021). Reverse phase encoded images were also acquired to enable distortion correction. For project one, the four task scans described above were used for data analyses. For project two, only resting state scans were used for these analyses: sequences of 500 volumes were acquired from all subjects with eyes open, staring at a fixation cross displayed on a screen.

Data were preprocessed with the Analysis of Functional NeuroImages (AFNI) (Cox, 2012), FreeSurfer (Fischl, 2012), and FMRIB Software Library (FSL) (Jenkinson, Beckmann, Behrens, Woolrich, & Smith, 2012) packages based on scripts provided by the 1000 Functional Connectome Project (Biswal et al., 2010). The parameters for preprocessing were retained from the parent study (Lim et al., 2020).

The T1 anatomical image was preprocessed using FreeSurfer's autorecon1 sequence, which includes motion correction, intensity normalization, and Talairach transformation. A mask was then generated for stripping the skull away from the image, leaving only brain; this mask was reoriented to match the original scan then used to crop it. This skull-stripped image was retained for later use.

All functional data including resting state and task scans were preprocessed using the same steps. First, they were corrected for field map distortion using FSL's topup. Next, the first five volumes were discarded for signal equilibrium, then the data were corrected for motion via Fourier interpolation. At this point, six motion parameters were calculated for the subject's rotational movement around three degrees of freedom (pitch, yaw, and roll axis), and cardinal directional movement in the x-, y-, and z-planes. Then, the skull was stripped, the data were

aligned with the mean, and the eighth image of the mean-aligned data was extracted for registration. After that, spatial smoothing was performed using a Gaussian kernel with a full width at half maximum of 6 mm, and the voxels were intensity-normalized, temporally filtered (0.005–0.3Hz), and detrended. Measures of motion outliers based on framewise displacement (FD) and the derivative of variability across voxels (DVARS) were then calculated using previously published methodology (Power, Barnes, Snyder, Schlaggar, & Petersen, 2012). Next, nuisance time courses for the global signal, cerebrospinal fluid, and white matter were calculated using masks from the image segmentation of the participant's T1-weighted data with a tissue-type probability threshold of 80%. These nuisance signals, along with the six motion parameters, were then removed by regression in native functional space. Functional images were then registered to the Montreal Neurological Institute (MNI-152) standard template using FMRIB's Linear Image Registration Tool (FLIRT) in three steps: 1) registering the native-space structural image to the MNI152 2mm template using a 12 degree of freedom linear affine transformation; 2) registering the native space functional image to the high-resolution structural image with a six degree of freedom linear transformation; 3) computing native functional to standard structural warps by concatenating the matrices computed in the first two steps.

For data quality verification, maximum FD and outlier rates for FD and DVARS were calculated to assess and exclude participants with high motion. Participant data with maximum FD above 3 mm or outliers in more than 30% of the acquired data were removed from the analysis (Saghayi et al., 2020). During the first study, some participants' scans had to be excluded, due to FD values exceeding 3 mm: subjects' neuroimaging data were excluded from two training scans (maximum FD = 3.61 and 5.19 mm) and two task scans (maximum FD = 4.35 and 5.86 mm). No scans were excluded based on outlier rate, as the highest percentage in our

dataset was 9.64%. For the second study, no participants were excluded because of these thresholds: in the HC data, the highest maximum FD obtained and highest percentage of outliers in data detected for all participants were 2.62 mm and 11.74%, respectively; in the CBP dataset, the maximum FD and percentage of outliers in data were 2.57 mm and 8.10%, respectively, for the first resting state scan, and 1.86 mm and 7.09%, respectively, for the second.

2.5. Brain Parcellation

We divided the brain's spatial domain into a set of non-overlapping regions using an optimized Harvard-Oxford parcellation with 131 regions that has been previously used in the lab (Hashmi et al., 2017; Saghayi et al., 2020; Wang et al., 2022). However, since our main seed regions of interest (ROIs) were the shell and core of the NAc, we replaced the bilateral whole-NAc regions provided by the Harvard-Oxford parcellation with four ROIs representing the left and right shell and core from a parcellation scheme derived from diffusion tractography (Cartmell et al., 2019), as they closely matched the regions demarcated by immunohistochemistry.

To make these new ROIs compatible with the rest of the dataset and ensure no overlap, the original masks provided by Cartmell et al. (2019) were used as a reference to draw new masks using edit mode in FSLeyes and the following parameters: 1) 3D voxel mode, 2) selection size=1, 3) MNI 2 mm^3 standard space, 4) lower threshold cut-off of 0.495, and 5) upper threshold cut-off of 0.900. This resulted in ROIs with 14 voxels for the left core, 28 voxels for the right core, 43 voxels for the left shell, and 50 voxels for the right shell. The (x, y, z) coordinates for the left core were (-10.2, 14.3, -6.9), right core (11.6, 15.7, -7.4), left shell (-8.2, 9.9, -9.2) and right shell (7.5, 9.8, -8.7) in MNI space. These masks had very similar coordinates

to other studies parcellating the human NAc shell and core (M. N. Baliki et al., 2013; S. H. Xia et al., 2020; X. Xia et al., 2017).

2.6. Data Analyses

For project one, behavioural data analyses first included a three-factor general linear model (matched cue vs. cue reversal X high vs. low temperature X static vs dynamic stimuli) to test for differences in pain perception in response to cue reversals and different stimuli characteristics. To test for the specific within-subjects differences in pain ratings, paired t-tests were then used to assess significance. Specifically, pain ratings were compared between high and low temperatures and between static and dynamic stimuli for the uncued, matched, and mismatched conditions to determine whether pain perception was altered by temperature and stimulus characteristics. Next, delta-pain rating – the difference in pain rating during the high and low temperatures – for dynamic and static stimuli was calculated. These values were then compared between uncued and matched conditions for each stimulus type to assess whether cues affected pain ratings. Pain ratings between the matched condition and positive and negative expectation conditions were compared in static and dynamic trials to determine if expectation effects were present. These expectation effects were then compared between static and dynamic stimuli to determine any differences in expectation effects between the two stimuli. Finally, to assess whether individual participants responded to cueing effects, we binarized each participant into either ‘responders’ or ‘non-responders’ based on their responses to positive and negative expectation effects relative to baseline (i.e., matched expectation). We took the difference in pain ratings between the positive and matched expectation conditions, as well as between the negative and matched expectation conditions, then divided them by the participants’ pain score in the matched expectation condition and multiplying by 100. Our cutoff value for assigning a

participant to the responder condition was -20% for the positive expectation condition and 20% for the negative expectation condition.

Analyses of neuroimaging data for project one first included tests for differences in whole NAc activation in an overall repeated measures 3 X 2 X 2 ANOVA (cue vs. heat vs. rating X static vs. dynamic X high vs. low temperature). Nucleus accumbens activation was measured as a percent deviation above or below the mean NAc BOLD response across the whole scan. As well, the main effect of laterality was tested (left NAc vs. right NAc); if this was not significant, the analyses would focus on the right NAc. For cueing effects, NAc activation was averaged across all unknown cue epochs, all high cues, and all low cues separately and compared using paired t-tests. Average NAc activation during heat and rating events in the separate conditions (static and dynamic stimuli; high and low temperatures) were compared between the unknown, matched, and mismatched condition. Nucleus accumbens activation during cue, heat, and rating events in the static and dynamic high temperature conditions were tested in the right shell and core separately (to assess differential subregion activation during expectation effects) using paired t-tests. This is a hypothesis driven ROI-based analysis, where the NAc and its subregions were of specific interest. This contrasts the alternative first level analysis using a general linear model, where statistics are done voxel-wise using the whole brain, with the assumption that signals from each voxel are independent of one another. Additionally, to determine which psychological variables were important in NAc activation during heat and rating events, select variables (PCS and its subscales, FFMQ, state and trait anxiety, and BDI) were correlated with right NAc activation in the mismatched conditions (i.e., high cue-low temperature and low cue-high temperature). This correlation matrix was calculated using Pearson's R-values and corrected for multiple comparisons.

For project two, questionnaire responses and demographic data were compared groupwise between HC and CBP participants via independent-samples t-tests. Equality of variances were checked with Levene's test; if any comparisons failed, then appropriately adjusted statistics were reported. For neuroimaging analyses, BOLD time series were extracted from each voxel within each region and averaged, resulting in 133 time series for each participant. The four NAc shell and core time series were correlated with the other 129 regions to create 4x129 correlation matrices that described rsFC. Within- (shell > core and core>shell) and between-subjects (HC > CBP and CBP > HC) contrasts were tested. Within-subjects effects (shell vs. core) were tested in HC and CBP groups separately via paired t-tests, these were corrected for multiped comparisons at $p < 0.05$. Between-subjects analysis (CBP > HC and HC > CBP) was performed using an Analysis of Covariance (ANCOVA) with a 2 X 2 factorial design (HC/CBP X shell/core) in the left and right NAc separately with age as a covariate of no interest. Significant effects were then investigated with paired-samples t-tests at $p < 0.05$ and corrected for multiple comparisons with FDR at $q < 0.05$. Brain figures presented in the results were created using BrainNet Viewer (M. Xia, Wang, & He, 2013). Each brain region was considered as a node, and their pairwise connections (edges) represented the connection pathways between different regions (Smith et al., 2013). To describe the brain subnetworks involved in shell and core connectivity and their differences between HC and CBP patients, we determined whether the significant nodes as defined by surviving whole-brain correction from the rsFC analysis above belonged to one of the five canonical RSNs: 1) subcortical, 2) salience, 3) default mode, 4) attention/executive, and 5) language/memory, as described previously (Hashmi et al., 2017; Saghayi et al., 2020).

Planned sub-analyses based on the significant outcomes of the CBP > HC and CBP < HC contrasts were completed to determine whether these connections could predict clinical behavioural measures in CBP patients, specifically BPI and NPS pain intensity scores. To correct for multiple comparisons, FDR $q < 0.10$ was sued as a cut-off to; Pearson's correlations were then performed on any significant findings that surpassed the FDR threshold between these connections and BPI and CBP pain intensity scores. Since the statistics relied on one resting state scan in HCs and the mean of two resting state scans in CBP, tests were done to determine whether the clinically relevant NAc network could also be observed when comparing HC and the two CBP resting state scans (i.e., HC vs. rest 1 CBP and HC vs. rest 2 CBP). Additionally, to test the sensitivity and specificity of the significant CBP > HC rsFC values in distinguishing the two groups, we plotted receiver operator characteristic (ROC) curves and calculated the area under the curve (AUC) for each functional connectivity contrast. The threshold was set at 0.7 for the AUC to deem the differences as meaningful, as this threshold is considered acceptable in determining the ability to distinguish between two groups (Mandrekar, 2010). For ROC curve analyses, AUC was calculated for each functional connectivity contrast: AUC > 0.9 was considered a good predictor, AUC > 0.7 was considered a moderate predictor, and AUC < 0.7 was considered a weak predictor. Finally, an out of sample group of CBP and HC participants were used as a validation dataset to check if the initial CBP > HC and CBP < HC results reproduced in a separate dataset.

CHAPTER 3. Results

3.1. Demographics

For project one, 35 healthy adults were recruited (21 females; age = 27.31 years ± 1.89 SEM). Five participants were used as pilot data; they completed all testing outside the MRI scanner. The remaining participants completed the experimental protocols inside the scanner. For project two, healthy controls and CBP participant demographics are described in Table 3. 1.; clinical characteristics of the CBP group are described in Table 3. 2. Behavioural and neuroimaging data from 41 HC (22 females) and 57 CBP patients (39 females) were used in analysis. Additionally, in the validation dataset, out of sample resting-state data from 30 HC (18 females, age = 27.6 years ± 2.12) and 18 CBP patients (15 females) were used. Demographic data for the CBP validation dataset is provided in Table 3. 3.

Parameter	***n***		**Mean ± SEM**		***t*-stat**	***p*-value**
	CBP	HC	CBP	HC		
Age	57	41	43.02 ± 1.82	31.76 ± 1.55	4.713	< 0.001
PCS	52	41	21.40 ± 1.37	12.59 ± 1.56	4.250	< 0.001
BDI-II	52	41	15.42 ± 1.40	5.90 ± 0.86	5.806	< 0.001

Table 3. 1. Clinical demographic parameters comparing CBP with HC. *Abbreviations:* BDI-II, Beck Depression Inventory-II; CBP, chronic back pain; HC, healthy controls; PCS, Pain Catastrophizing Scale; SEM, standard error of the mean.

Parameter	***n***	**Mean ± SEM**
Time since diagnosis (years)	40	7.48 ± 0.98
Duration of treatment (years)	40	7.05 ± 0.84
MPQ Sensory	52	15.90 ± 0.85
MPQ Affective	52	4.88 ± 0.40
NPS Total	52	46.25 ± 1.74
NPS Pain Intensity	52	59.04 ± 2.82
BPI Average Pain	53	51.74 ± 2.12
BPI Total Areas of Pain	57	7.42 ± 0.71
MQS	54	6.61 ± 0.88

Table 3. 2. Chronic back pain specific clinical measurements. *Abbreviations:* BPI, Brief Pain Inventory; MPQ, McGill Pain Questionnaire; MQS, Medication Quantification Scale; NPS, Neuropathic Pain Scale; SEM, standard error of the mean.

Parameter	*n*	Mean±SEM
Age	17	36.1±2.75
PCS	15	25.13±2.60
BDI-II	15	20.47±2.88
Time since diagnosis (years)	9	5.8±1.50
Duration of treatment (years)	10	6.32±1.70
MPQ Sensory	15	15.93±0.87
MPQ Affective	15	5.27±0.61
NPS Total	15	42.73±2.80
NPS Pain Intensity	15	60±3.65
BPI Average Pain	15	57±2.52

Table 3. 3. Demographic data for the chronic back pain patients in the validation dataset. *Abbreviations:* BPI, Brief Pain Inventory; MPQ, McGill Pain Questionnaire; MQS, Medication Quantification Scale; NPS, Neuropathic Pain Scale; SEM, standard error of the mean.

3.2. Project One Behavioural Results

3.2.1. Pain Perception is Influenced by Matched Expectation Cues Similarly for Static and Dynamic Heat

First, it was established that expectation cues had a significant influence on pain ratings. The extent to which presentation of low and high threat cues influenced pain ratings relative to uncued threat cues was evaluated. The presentation of cues significantly increased the difference between pain response evoked by the the 45°C and 47°C stimulus relative to the uncued trials (Figure 3. 1.) for both static (difference = 35.55 ± 3.31 for cued, 25.63 ± 2.69 for uncued; $t(34) = 3.871$, $p < 0.001$) and dynamic (difference = 44.65 ± 2.98 for cued, 36.54 ± 2.75 for uncued; $t(34) = 3.413$, $p = 0.002$) stimuli. Therefore, pain responses to low temperatures (45°C) decreased and to high temperatures (47°C) increased when paired with low and high threat cues, respectively, for both static and dynamic stimuli. Overall, pain ratings became aligned with the

two types of cues (15% and 90% intensity) and the difference between high and low temperatures was less pronounced in the uncued conditions, suggesting top-down effects. This effect was not specific to stimulus type and was observed in both static (difference in pain ratings between uncued and matched cue conditions, 9.92 ± 2.56) and dynamic stimuli (8.12 ± 2.38; $t(34) = 0.722$, $p = 0.475$), suggesting that cueing the stimuli normalized any differences in pain response between static and dynamic stimuli. As well, in the uncued condition, pain ratings were significantly higher in the dynamic stimuli compared to the static stimuli, suggesting that despite equivalent peak temperature, the dynamic increase in heat stimuli evoked a higher pain rating (See Table 3. 4.).

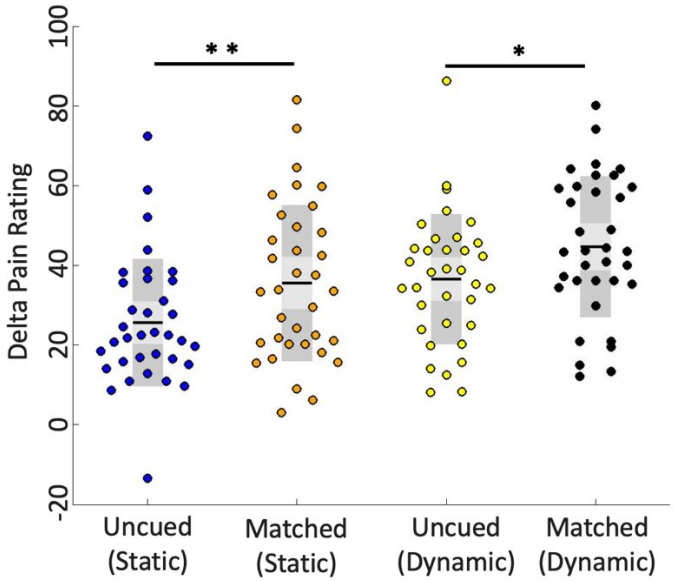

Figure 3. 1. Depiction of the difference in pain intensity responses (high – low temperature) between matched and uncued conditions. Pain rating differences were higher during the uncued trials relative to the matched trials. *Note.* * $p < .01$, ** $p < .001$.

3.2.2. Static Stimuli Generated Greater Expectation Effects Relative to Dynamic Stimuli

Next, it was found that cue reversal impacted pain perception. Cue reversals were introduced where low cues (1-20%) corresponded with the high temperature (47°C) and high

cues (80-100%) corresponded with the low temperature (45°C) in both the static and dynamic conditions (Figure 3. 2. A-B).

Analysis revealed significantly lower pain ratings during the positive expectation epochs (low cue paired with 47°C) relative to matched expectation epochs (high cue paired with 47°C) for both the static ($t(34) = 3.942$, $p < 0.001$) and dynamic ($t(34) = 3.333$, $p = 0.002$) conditions (see Table 3. 4. for mean pain ratings). However, there were no significant differences in pain ratings during negative expectation (high cue paired with 45°C) epochs in either the static ($t(34) = 1.547$, $p = 0.131$) or dynamic ($t(34) = 0.211$, $p = 0.834$) conditions. This difference was significant during positive but not negative expectations.

To compare the effects of expectations on pain between static and dynamic stimuli, the effect of difference between pain ratings evoked by static and dynamic stimuli was normalized by using the differences in pain rating between matched and mismatched conditions and comparing these values (Figure 3. 2. C). There was a significant difference between static and dynamic expectation effects during positive (low cue paired with 47°C; static = -7.35 ± 1.23, dynamic = -2.47 ± 1.02; $t(34) = 5.120$, $p < 0.001$), but not negative (high cue paired with 45°C; static = 2.24 ± 1.15, dynamic = 1.53 ± 1.08, $t(34) = 0.614$, $p = 0.543$) expectations; affirming that the static condition produces greater expectation effects compared to the dynamic condition.

In addition, expectation effects were observed in a greater number of participants during static, relative to dynamic, stimuli. During positive expectation epochs, there were 18/35 (51%) responders in the static condition and 5/35 (14.2%) responders in the dynamic condition. During the negative expectation condition, there were 16/35 (45.7%) responders in the static condition and 15/35 (42.85%) responders in the dynamic condition. This suggests that positive expectations significantly influenced responses to static stimuli relative to dynamic stimuli.

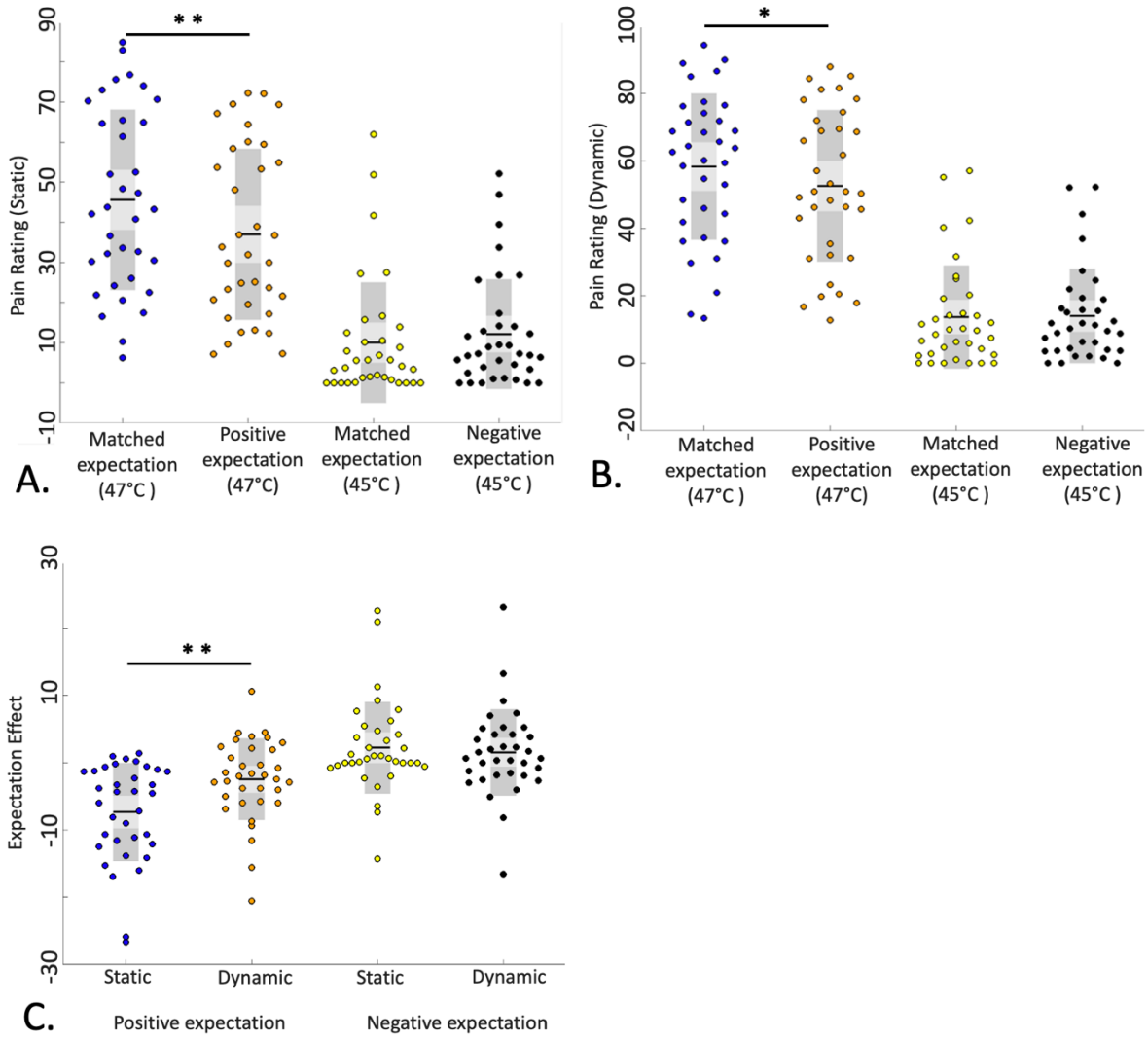

Figure 3. 2. Schematic representing the main behavioural results of the study paradigm, highlighting greater expectation effects produced in static relative to dynamic stimuli during positive expectation. **A.** Pain ratings were lower during the positive expectation condition relative to the matched (47°C) expectation condition; no such effect was observed between the negative expectation compared to the matched (45°C) condition during the static epochs. **B.** Positive and negative expectation effects produced similar outcomes as those in Panel A during dynamic epochs as well. Overall, positive expectation, but not negative expectation, significantly biased pain ratings in both the static and dynamic epochs. **C.** Differences in expectation effects between static and dynamic stimuli were calculated by taking the difference between cued epochs and cue reversals during both positive (low cue high temperature – high cue high temperature) and negative (high cue low temperature – low cue low temperature) expectation epochs.

Positive, but not negative, expectation effects were significantly different between static and dynamic temperatures.

Note. * p < .01, ** p < .001.

Condition	Stimulus Characteristics	Mean ± SEM	Paired *t*-test	*p*-value
Uncued	Static (45°C)	14.75 ± 2.70		
	Static (47°C)	40.39 ± 3.22	$t(34) = 9.529$	$p < .001$
	Dynamic (45°C)	15.65 ± 2.76		
	Dynamic (47°C)	52.19 ± 3.47	$t(34) = 13.292$	$p < .001$
Matched	Static (45°C)	10.05 ± 2.54		
	Static (47°C)	45.60 ± 3.80	$t(34) = 10.742$	$p < .001$
	Dynamic (45°C)	13.64 ± 2.58		
	Dynamic (47°C)	58.29 ± 3.66	$t(34) = 14.986$	$p < .001$
Positive expectation	Static (47°C)	37.00 ± 3.60		
	Dynamic (47°C)	52.56 ± 3.80	$t(34) = 10.290$	$p < .001$
Negative expectation	Static (45°C)	12.13 ± 2.30		
	Dynamic (45°C)	13.96 ± 2.35	$t(34) = 2.054$	$p = .048$

Table 3. 4. Pain ratings were significantly higher during the 47°C stimuli relative to the 45°C stimuli within the cued and uncued conditions, in both the static and dynamic conditions. As well, pain ratings were significantly higher in the dynamic condition relative to the static condition within the same temperature. *Abbreviation:* SEM, standard error of the mean.

3.3. Neuroimaging Results – Expectation Effects on Static vs Dynamic Stimuli (Study 1)

First, to test for activation differences between the left and right NAc, the main effect of laterality was tested and was not significant, ($F(1,27) = 1.047$, $p = 0.827$). Therefore, analyses focused on the right NAc (contralateral to thermal stimulation) for further analyses. The mean nucleus accumbens activation for durations when the heat and the rating scale was presented were entered into a model to test for the effects of different conditions in a repeated measures ANOVA (see methods section 2.6). The overall ANOVA was significant ($F(4,24) = 4.630$, $p = 0.019$). As well, shell and core effects were analyzed separately and significant effects were

found, the dynamic stimulus held at 47°C produced significant differences in responses between the uncued, matched and mismatched conditions to heat (details provided in section 3.3.3.).

3.3.1. Nucleus Accumbens Activation Across Conditions

3.3.2. Effects of Different Cueing Conditions on NAc Activation During Cue Presentation

Countering evidence of increased NAc response to rewarding cues in humans (Knutson, Wimmer, Kuhnen, & Winkielman, 2008), in this model where aversive and uncertain cues were presented, there were no significant differences in whole or subregion NAc activation to changing cues. Right nucleus accumbens activation averaged for the duration of cue presentation for low heat cues (-7.79 ± 1.89; percent deviation from the mean) was similar to activation to high heat cues (-6.89 ± 2.10) and for unknown cues (-6.16 ± .83; $p > 0.05$).

There NAc subregion (shell and core) activation to cues also did not differ between low heat cues (-9.07 ± 1.36), unknown cues (-5.26 ± 1.32), and high heat cues (-6.54 ± 1.53). Similarly, there was no difference in activation in the right shell across low heat cues (-4.44 ± 1.14), unknown cues (-1.83 ± 1.07), and high heat cues (-3.15 ± 1.26).

3.3.3. NAc Response to Heat

Whole NAc responses were tested for differences during heat across static and dynamic and high and low temperatures (Figure 3. 3.). During heat, NAc activation was significantly higher in the uncued (11.37 ± 1.69; $t(27) = 3.425$, $p = 0.002$) and positive expectation (9.77 ± 1.66; $t(27) = 2.244$, $p = 0.033$) condition relative to the matched expectation (4.39 ± 2.13) condition during the dynamic high condition, indicating that the NAc responds to motivational salience of stimuli.

There was no significant effect (p's > 0.05) of uncued (3.39 ± 2.20), matched expectation (6.15 ± 1.48), or positive expectation (6.03 ± 1.46) during heat in the static high condition.

During static low epochs, NAc activation did not significantly differ during heat across uncued (10.69 ± 2.50), matched expectation (7.16 ± 1.68), or negative expectation (9.69 ± 1.84). During the dynamic low epochs, NAc activation did not differ across uncued (7.74 ± 1.31), matched expectation (5.04 ± 2.13), or negative expectation (3.78 ± 1.53), although NAc activation during the uncued epochs was higher than the negative expectation condition and was approaching significance ($t(29) = 2.047$, $p = 0.050$).

Because the high temperatures produced the most robust results, we focused on the high temperatures across the static and dynamic stimuli for the NAc subregion analysis (Figure 3. 4.). In the dynamic epochs, the mean activation in the right core during heat in the uncued condition (11.55 ± 1.65) was significantly higher ($t(29) = 4.635$, $p < 0.001$) relative to the training condition (0.70 ± 1.92). As well, the positive expectation condition (8.48 ± 1.60) produced significantly higher ($t(29) = 3.248$, $p = 0.003$) mean activation relative to the matched condition. There was no difference between the uncued and positive expectation condition. In the right shell, no effects were observed between the uncued (7.45 ± 1.54), matched (3.76 ± 1.81), or positive expectation (6.33 ± 1.41) conditions.

Across the static (47°C) epochs, no effects were observed in the activation of the right core (p's > 0.05) during heat between the uncued (1.82 ± 2.59), matched (5.92 ± 1.68), and positive expectation (5.48 ± 1.51) condition. No effects were observed in the right shell when comparing the mean heat activation between the uncued (1.87 ± 1.79), matched (3.81 ± 1.16), and positive expectation (3.37 ± 1.32).

Overall, the core is specifically involved in encoding uncertainty and prediction error during heat, and that this is specific to dynamic, not static, stimuli.

3.3.4. NAc Response to Rating

During rating in the static high epochs, the NAc showed a decrease in activation during the uncued (-5.91 ± 1.54) condition relative to the matched (-0.87 ± 1.39; t(29) = 2.853, p = 0.008) and positive expectation (1.16 ± 2.15; t(29) = 3.410, p = 0.002) conditions. During rating in the dynamic high epochs, there were no significant differences (p's > .05) between the uncued (-7.19 ± 1.95), matched expectation (-7.02 ± 2.12), or positive expectation (-6.45 ± 1.99) conditions. During rating in the static low temperature events, the matched expectation (5.87 ± 2.08) condition produced higher NAc activation relative to the negative expectation (1.10 ± 1.93; t(29) = 2.154, p = 0.040) and uncued (1.07 ± 1.81; t(29) = 2.092, p = 0.045) conditions. During rating in the dynamic low epochs, no comparisons were significant between the uncued (-0.65 ± 1.91), matched (-1.99 ± 2.17), and negative expectation (-1.33 ± 1.68) conditions. Overall, during rating, both the core and shell seem to be de-activated during the uncued condition; this is specific to the static epochs.

During rating after the static (47°C) stimuli, the mean activation in the right core was significantly higher (t(29) = 3.727, p < 0.001) in the positive expectation condition (3.11 ± 2.49) relative to the uncued condition (-5.68 ± 1.78). No other differences were observed, mean activation in the matched condition was (-1.20 ± 1.73). In the right shell, the unknown condition (-6.16 ± 1.43) had significantly more de-activation relative to the matched condition (-1.95 ± 1.33; t(29) = 2.796, p = 0.009) and positive expectation condition (-0.99 ± 1.95; t(29) = 2.349, p = 0.026).

During the dynamic epochs, no differences in mean activation were observed in the right core activation between the unknown (-5.74 ± 2.03), matched (-5.92 ± 2.12), and positive expectation (-4.73 ± 1.85) conditions. In the right shell, no differences in mean activation were

observed between the unknown (M = -7.89 ± 1.94), matched (-7.58 ± 2.13), and positive expectation (-7.15 ± 1.88) conditions.

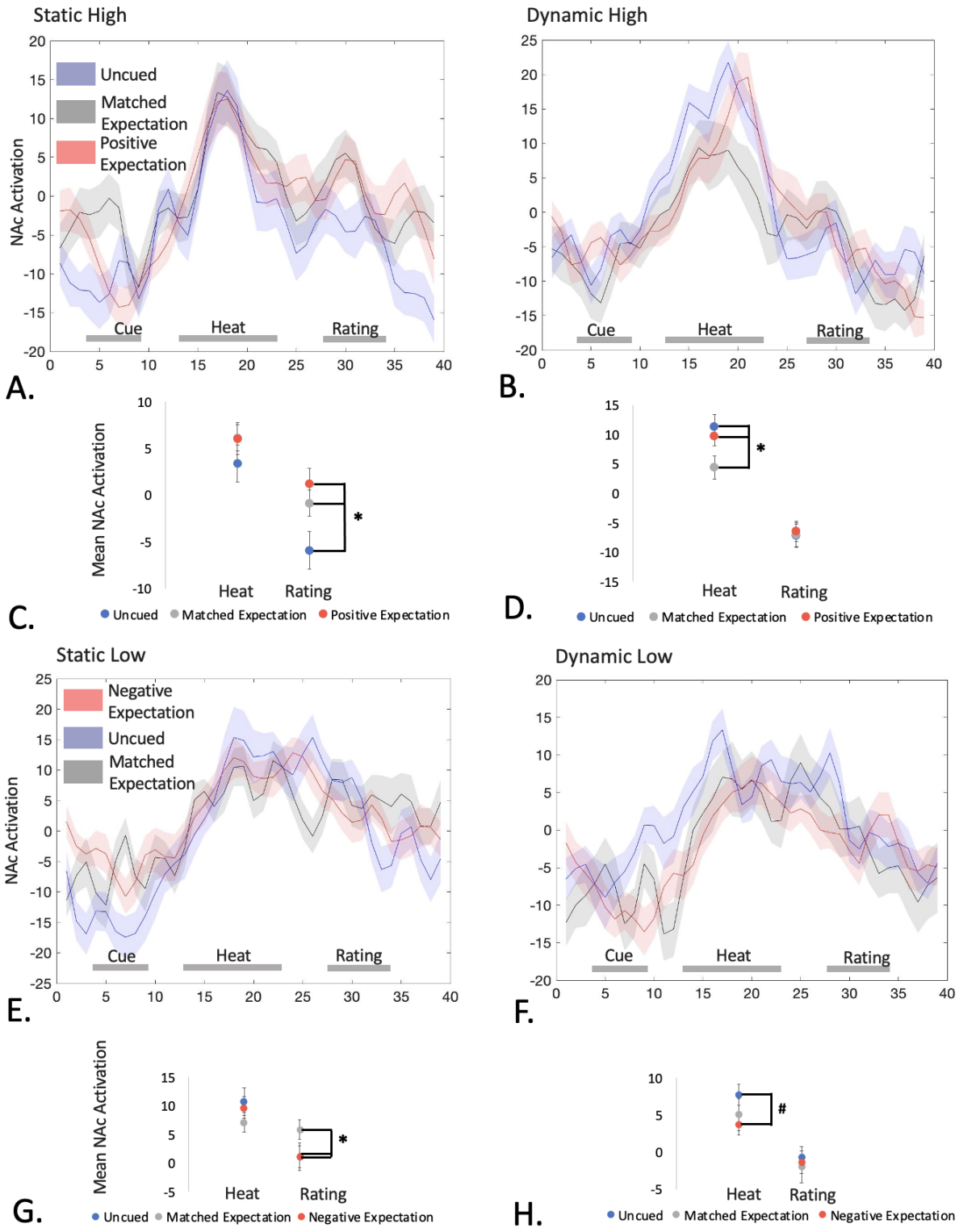

Figure 3. 3. The right NAc activations plotted during the task scans across time, separated by high and low temperature, and static and dynamic stimuli. Differences in mean NAc response during heat and rating were analyzed; averages of the NAc activations are plotted below the NAc activation timeseries graphs. **A.** Plot of the

NAc activations during the uncued, matched, and positive expectation conditions during the static high temperature epochs. **B.** Represents the NAc activations during the dynamic high conditions. **C.** Differences in mean NAc activation were compared during heat and rating periods. In the static high epochs, the average activations during heat were not different from each other, but the activations during rating were higher in the positive and matched expectation condition compared to the uncued condition. **D.** During the dynamic high epochs, mean NAc activations were significantly higher in the uncued and positive expectation condition relative to the matched expectation condition; no effects were found during the rating event. **E.** Depicts the NAc activations during the uncued, matched and negative expectation during static low epochs. **F.** Represents the NAc activations during the dynamic low conditions. **G.** We assessed the mean activation differences during the heat and rating events; no differences were observed during heat events in the static low condition. During rating, mean NAc activity was higher during matched expectation compared to negative expectation and uncued conditions. **H.** No significant differences were observed during heat or rating in the dynamic low condition, although the uncued mean activation was trending towards significance when compared to the negative expectation condition during heat. Note. * $p < 0.05$, # $p = 0.050$.

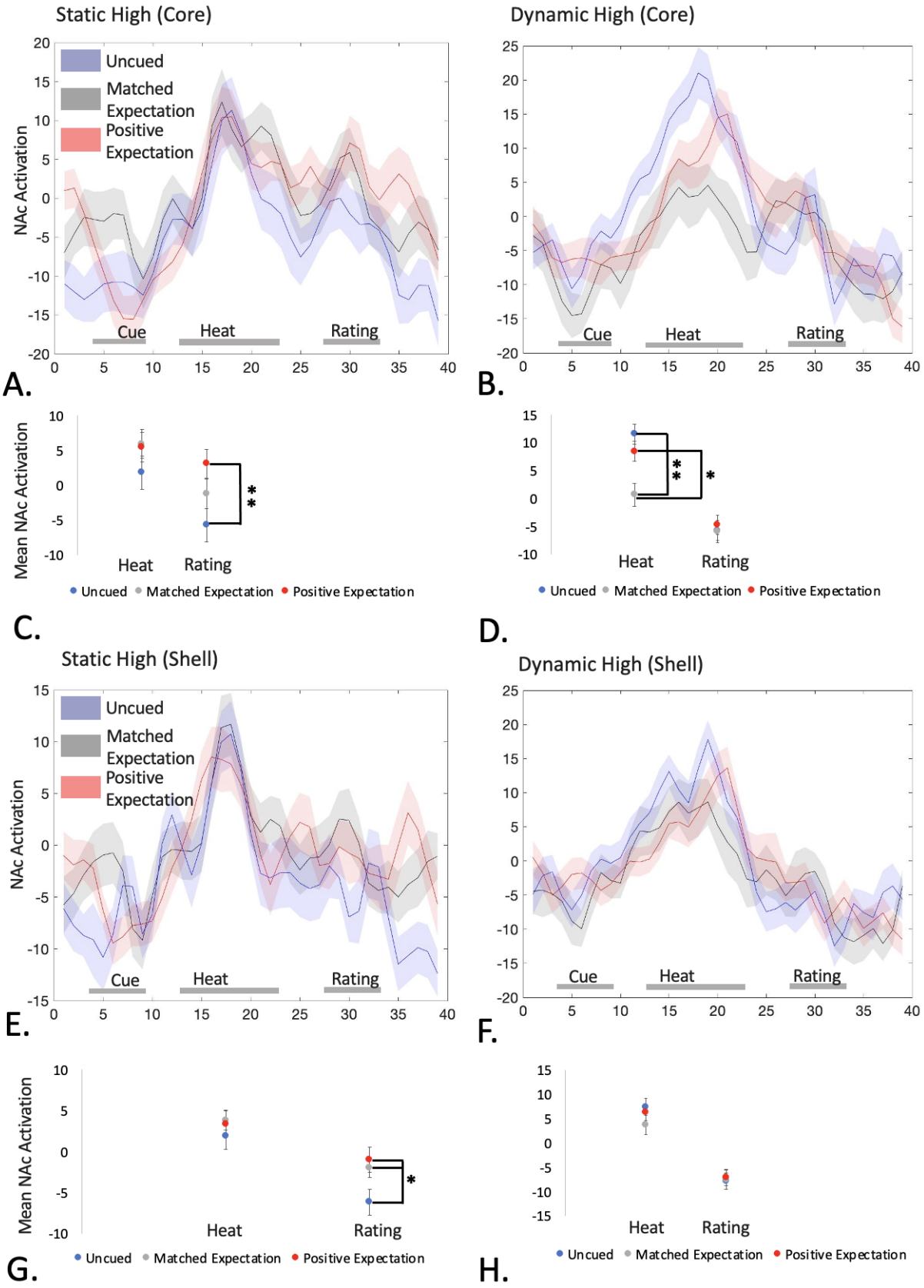
Static High (Core)
Uncued
Matched Expectation
Positive Expectation
NAc Activation
Cue
Heat
Rating
A.
Dynamic High (Core)
B.
Mean NAc Activation
Heat
Rating
Uncued
Matched Expectation
Positive Expectation
C.
D.
Static High (Shell)
E.
Dynamic High (Shell)
F.
G.
H.

Figure 3. 4. The NAc core and shell activations during the static and dynamic high temperature conditions; mean activation during heat and rating was assessed. **A.** The NAc timeseries graph in the NAc core during static high epochs during the uncued, matched, and positive expectation conditions. **B.** Graph of the NAc core activation during the dynamic high conditions. **C.** Mean activation in the core during static epochs was significantly higher in the positive expectation condition relative to the uncued condition during rating; no effects were observed during heat. **D.** During dynamic epochs, mean core activation was higher in the uncued and positive expectation conditions relative to the matched expectation condition; no effects were observed during rating. **E.** NAc shell timeseries during the static high conditions. **F.** Graph of the NAc shell activations during the dynamic high conditions. **G.** Both the positive and matched expectation conditions had less deactivation relative to the uncued condition in the shell during rating. **H.** No heat or rating effects were observed in the shell during the dynamic high condition. Note. * $p < 0.05$, ** $p < 0.01$

3.3.5. Association between NAc activation and psychological parameters

After correction for multiple comparisons (FDR $q < 0.05$), there were significant correlations between NAc response and affective measures. Thus, mean activation in the right NAc during heat and rating events were correlated with scores on behavioural questionnaires during heat and rating events and results are presented in Table 3. 5.

During rating events in the dynamic epochs, NAc activity was positively correlated with depression and anxiety, but negatively correlated with the nonjudgmental subscale of the FFMQ in the negative expectation condition. These correlations were reversed during the rating period for positive expectation; depression and anxiety were negatively correlated with NAc activity and the FFMQ was positively correlated with NAc activity.

During the heat events in the negative expectation condition, NAc activity was positively correlated with depression and anxiety scores during heat in the static condition, but not in the dynamic condition. The NAc response to heat was instead associated with the observing subscale of the FFMQ during the dynamic condition. Overall, these results reveal that psychological

measures are associated with NAc activity during heat and rating that differs between negative and positive expectation. No other conditions were significant with these psychological measures.

	Negative Expectation (Static Heat)	**Negative Expectation (Dynamic Heat)**	**Negative Expectation (Dynamic Rating)**	**Positive Expectation (Dynamic Rating)**
BDI	.442*	.031	.579**	-.579**
State Anxiety	.413*	.315	.516**	-.567**
Trait Anxiety	.455*	.140	.566**	-.614***
FFMQ	-.380	-.056	-.353	.532**
FFMQ Awareness	-.354	-.075	-.368	.517**
FFMQ Nonjudgmental	-.533	-.382	-.493**	.710***
FFMQ Observing	.273	.422*	.126	-.171

Table 3. 5. Correlation matrix of the measures that significantly correlated with the right NAc activation in the mismatched expectation conditions. Note: Numbers populating the correlation matrix represent Pearson's correlation coefficients; * $p < 0.05$, ** $p < 0.01$, *** $p < 0.001$. *Abbreviations:* BDI, Beck Depression Inventory; FFMQ, Five-Facet Mindfulness Questionnaire. Corrected for multiple comparisons.

3.4. Neuroimaging Results – NAc Connectivity Differences Within and Between Groups (Study Two)

3.4.1. NAc Resting State Functional Connectivity Differences Between the Shell and Core

In both HC and CBP patients, the core was more connected to regions within the subcortical, salience, and executive networks (Figure 3. 5. A-B), while the shell was significantly more connected to regions within the default mode, and language/memory networks (Figure 3. 5. C-D; whole brain corrected at $p < 0.05$). In HC, the left core and shell had fewer significant

edges (5 and 4, respectively) compared to the right core and shell (16 and 21, respectively); in CBP, the left core and shell had fewer significant edges (12 each) compared to the right core and shell (26 and 19, respectively). These distinctions in connectivity between core and shell, based on resting-state network, are further visualized in Figure 3. 5. E. Table 3. 6. provides a comprehensive list of all the significant regions found for each contrast of left and right shell and core connectivity in HC and CBP.

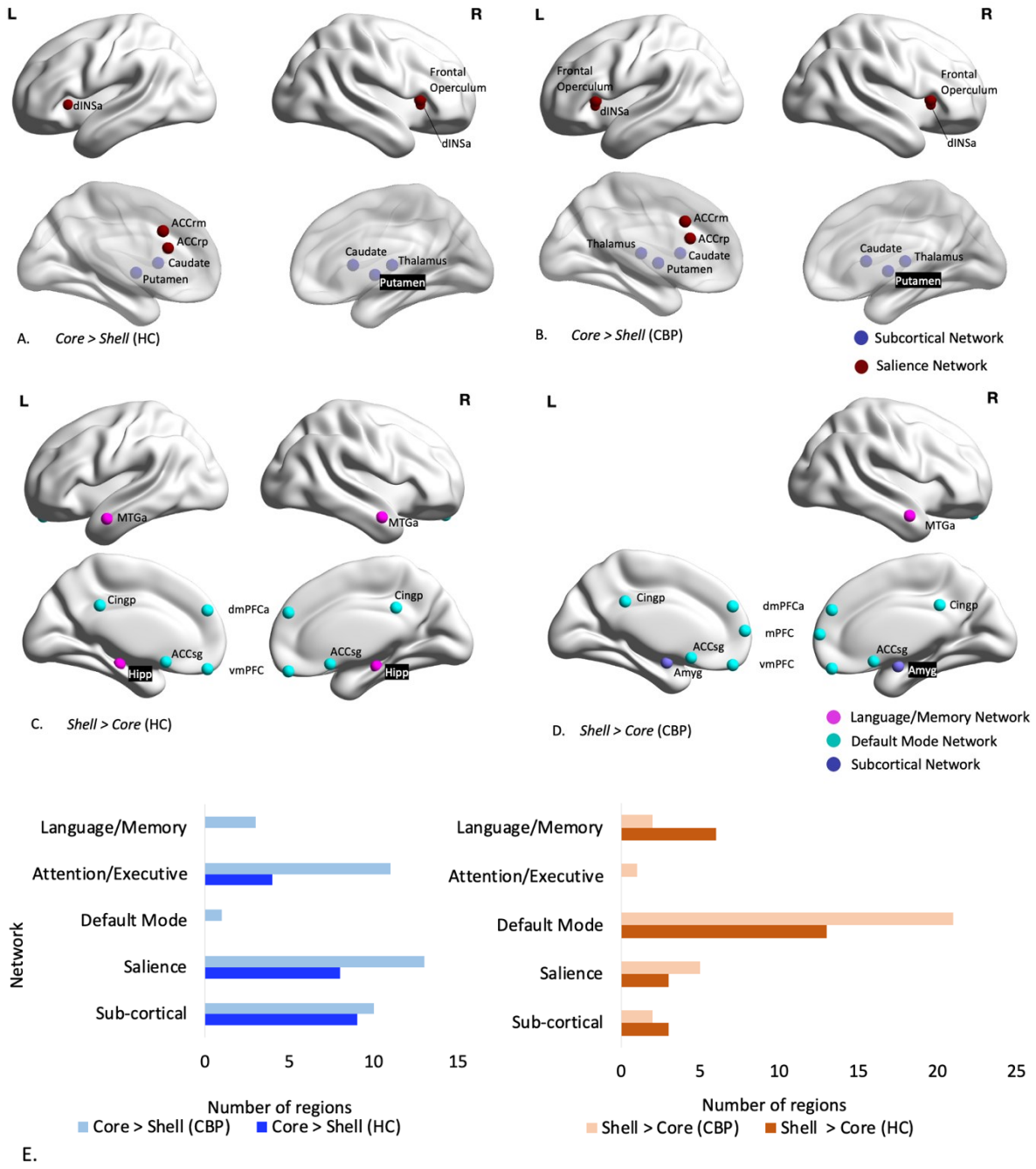

Figure 3. 5. Functional connectivity contrast analyses reveal differential connectivity of the NAc core and shell within healthy controls (HC) and chronic back pain (CBP) patients. **A**. The significant core > shell contrasts in HC, and **B.** in CBP patients. Overall, the core was more connected to subcortical and salience network regions in both groups. **C.** The significant shell > core contrasts in HC and **D.** in CBP patients. These show more connections to language, memory, and default mode network regions in the shell relative to the core in both groups. **E.** Each significant region was classified into one of five resting state networks, and the number of significant regions was

quantified for each contrast. Note: left and right brain images represent sagittal views; the top set are viewed from the lateral side while the bottom set are viewed from the medial side at the midbrain. Significances are whole brain corrected at $p < 0.05$. *Abbreviations:* ACCrm, rostral anterior cingulate cortex mid posterior; ACCrp, rostral anterior cingulate cortex posterior; ACCsg, subgenual anterior cingulate cortex; Amyg, amygdala; Cingp, cingulate gyrus posterior division; dINSa, dorsal anterior insula; dmPFCa, dorsal medial prefrontal cortex anterior division; Hipp, hippocampus; mPFC, medial prefrontal cortex; MTGa, middle temporal gyrus anterior division; vmPFC, ventromedial prefrontal cortex.

	Hemi.	**MNI coordinates (x, y, z)**	***t*-stat**	***p*-value**
Left Core > Left Shell (HC)				
Caudate	L	-12, 14, 8	10.48	< 0.001
Putamen	L	-30, -4, 0	7.88	< 0.001
Caudate	R	12, 14, 8	5.21	< 0.001
Putamen	R	30, -4, 0	4.32	< 0.001
Rostral anterior cingulate cortex mid posterior	L	-6, 18, 34	3.42	0.001
Left Core > Left Shell (CBP)				
Caudate	L	-12, 14, 8	13.46	< 0.001
Putamen	L	-30, -4, 0	6.32	< 0.001
Orbitofrontal pole	L	-32, 58, -6	4.06	< 0.001
Thalamus	R	10, -18, 8	3.48	0.001
Thalamus	L	-10, -18, 8	3.25	0.002
Supplementary motor area	R	4, -2, 58	3.09	0.004
Caudate	R	12, 14, 8	3.09	0.004
Dorsal anterior insula	L	-32, 20, 0	3.05	0.004
Frontal Operculum	L	-40, 20, 4	3.03	0.004
Frontal orbital cortex	L	-40, 30, -14	2.89	0.006
Supplementary motor area	L	-4, -2, 58	2.88	0.007
Putamen	R	30, -4, 0	2.68	0.011
Left Shell > Left Core (HC)				
Subgenual anterior cingulate cortex	L	-4, 16, -14	-7.41	< 0.001
Subgenual anterior cingulate cortex	R	4, 16, -14	-4.01	< 0.001
Hippocampus	L	-28, -22, -16	-3.95	< 0.001
Parahippocampal gyrus	L	-24, -32, -18	-3.47	0.001
Left Shell > Left Core (CBP)				
Subgenual anterior cingulate cortex	L	-4, 16, -14	-10.23	< 0.001

	Hemi.	MNI coordinates (x, y, z)	*t*-stat	*p*-value
Lateral occipital cortex	R	40, -78, 34	-5.38	< 0.001
Cingulate gyrus posterior division	L	-4, -38, 32	-4.47	< 0.001
Amygdala	L	-24, -4, -18	-4.28	< 0.001
Dorsal medial prefrontal cortex anterior division	R	4, 50, 28	-4.27	< 0.001
Subgenual anterior cingulate cortex	R	4, 16, -14	-3.98	< .001
Cingulate gyrus posterior division	R	4, -38, 32	-3.55	0.001
Temporooccipital middle temporal gyrus	R	60, -52, 0	-3.30	0.002
Lateral occipital cortex	L	-40, -78, 34	-3.07	0.004
Medial prefrontal cortex	R	6, 60, 8	-2.90	0.006
Precuneus	R	4, -64, 38	-2.87	0.007
Dorsal medial prefrontal cortex anterior division	L	-4, 50, 28	-2.79	0.008
Right Core > Right Shell (HC)				
Caudate	R	12, 14, 8	7.45	< 0.001
Putamen	R	30, -4, 0	7.04	< 0.001
Rostral anterior cingulate cortex mid posterior	R	6, 18, 34	5.79	< 0.001
Posterior supramarginal gyrus	R	60, -48, 32	4.82	< 0.001
Dorsal anterior insula	R	32, 20, 0	4.60	< 0.001
Anterior supramarginal gyrus	R	58, -32, 40	4.20	< 0.001
Frontal Operculum	R	40, 20, 4	3.61	0.001
Rostral anterior cingulate cortex mid posterior	L	-6, 18, 34	3.47	0.001
Inferior frontal gyrus, pars opercularis	R	54, 14, 16	3.22	0.002
Rostral anterior cingulate cortex posterior	R	4, 22, 20	2.80	0.008
Thalamus	R	10, -18, 8	2.78	0.008
Putamen	L	-30, -4, 0	2.78	0.008
Dorsolateral prefrontal cortex	R	40, 20, 44	2.76	0.009
Caudate	L	-12, 14, 8	2.66	0.011
Dorsal anterior insula	L	-32, 20, 0	2.55	0.015
Rostral anterior cingulate cortex posterior	L	-4, 22, 20	2.52	0.016
Right Core > Right Shell (CBP)				
Putamen	R	30, -4, 0	9.21	< 0.001
Caudate	R	12, 14, 8	3.93	< 0.001
Posterior supramarginal gyrus	L	-60, -48, 32	3.82	< 0.001
Frontal Operculum	R	40, 20, 4	3.58	< 0.001
Parietal Operculum	L	-48, -32, 20	3.56	0.001
Planum polare	L	-48, -4, -6	3.46	0.001
Superior temporal gyrus anterior division	L	-58, -4, -6	3.46	0.001
Putamen	L	-30, -4, 0	3.44	0.001
Inferior frontal gyrus pars triangularis	R	50, 30, 16	3.41	0.002

	Hemi.	MNI coordinates (x, y, z)	*t*-stat	*p*-value
Supramarginal gyrus, anterior division	L	-58, -32, 40	3.40	0.002
Superior temporal gyrus posterior division	L	-66, -26, 6	3.34	0.002
Planum temporale	L	-60, -22, 8	3.31	0.002
Rostral anterior cingulate cortex mid posterior	R	6, 18, 34	3.26	0.002
Brain Stem	-	0, -26, -28	3.24	0.002
Dorsal anterior insula	L	-32, 20, 0	3.22	0.003
Occipital fusiform gyrus	L	-28, -76, -14	3.18	0.003
Temporal occipital fusiform cortex	L	-34, -54, -16	3.08	0.004
Temporal Pole	R	40, 16, -30	2.86	0.007
Lateral occipital cortex, inferior division	L	-48, -78, -2	2.82	0.008
Middle Insula	L	-40, -2, -2	2.79	0.008
Dorsal anterior insula	R	32, 20, 0	2.78	0.008
Posterior supramarginal gyrus	R	60, -48, 32	2.74	0.009
Rostral anterior cingulate cortex mid posterior	L	-6, 18, 34	2.73	0.009
Inferior frontal gyrus, pars opercularis	R	54, 14, 16	2.72	0.010
Central Operculum	L	-48, -4, 8	2.69	0.010
Frontal Operculum	L	-40, 20, 4	2.64	0.012
Right Shell > Right Core (HC)				
Subgenual anterior cingulate cortex	R	4, 16, -14	-16.97	< 0.001
Subgenual anterior cingulate cortex	L	-4, 16, -14	-12.45	< 0.001
Ventromedial prefrontal Cortex	L	-4, 50, -20	-6.00	< 0.001
Ventromedial prefrontal Cortex	R	4, 50, -20	-5.63	< 0.001
Temporal fusiform cortex posterior division	L	-36, -16, -32	-4.64	< 0.001
Temporal fusiform cortex posterior division	R	36, -16, -32	-4.63	< 0.001
Medial prefrontal cortex	R	6, 60, 8	-4.24	< 0.001
Middle temporal gyrus anterior division	R	58, -2, -22	-4.20	< 0.001
Medial prefrontal cortex	L	-6, 60, 8	-4.02	< 0.001
Hippocampus	L	-28, -22, -16	-3.83	< 0.001
Middle temporal gyrus posterior division	R	62, -22, -18	-3.71	0.001
Dorsal medial prefrontal cortex anterior division	R	4, 50, 28	-3.39	0.002
Dorsal medial prefrontal cortex anterior division	L	-4, 50, 28	-3.35	0.002
Cingulate gyrus posterior division	L	-4, -38, 32	-3.19	0.003
Parahippocampal gyrus, posterior division	L	-24, -32, -18	-3.02	0.004
Cingulate gyrus posterior division	R	4, -38, 32	-2.80	0.008
Parahippocampal gyrus, anterior division	L	-24, -6, -34	-2.77	0.008
Hippocampus	R	28, -22, -16	-2.76	0.009
Precuneus	L	-4, -64, 38	-2.60	0.013
Middle temporal gyrus anterior division	L	-58, -2, -22	-2.58	0.014
Lateral occipital cortex	L	-40, -78, 34	-2.56	0.014

	Hemi.	MNI coordinates (x, y, z)	*t*-stat	*p*-value
Right Shell > Right Core (CBP)				
Subgenual anterior cingulate cortex	R	4, 16, -14	-17.31	< 0.001
Subgenual anterior cingulate cortex	L	-4, 16, -14	-12.46	< 0.001
Dorsal medial prefrontal cortex anterior division	R	4, 50, 28	-6.78	< 0.001
Dorsal medial prefrontal cortex anterior division	L	-4, 50, 28	-6.31	< 0.001
Precuneus	R	4, -64, 38	-6.24	< 0.001
Medial prefrontal cortex	L	-6, 60, 8	-6.02	< 0.001
Cingulate gyrus posterior division	L	-4, -38, 32	-5.22	< 0.001
Medial prefrontal cortex	R	6, 60, 8	-5.05	< 0.001
Cingulate gyrus posterior division	R	4, -38, 32	-5.02	< 0.001
Lateral occipital cortex	R	40, -78, 34	-4.79	< 0.001
Precuneus	L	-4, -64, 38	-4.68	< 0.001
Ventromedial prefrontal Cortex	L	-4, 50, -20	-4.19	< 0.001
Caudal anterior cingulate cortex	L	-4, 40, -2	-4.10	< 0.001
Ventromedial prefrontal Cortex	R	4, 50, -20	-3.99	< 0.001
Superior frontal gyrus	L	-22, 22, 54	-3.64	0.001
Postcentral Gyrus	R	54, -20, 46	-3.32	0.002
Lateral occipital cortex	L	-40, -78, 34	-3.20	0.003
Amygdala	R	24, -4, -18	-3.18	0.003
Middle temporal gyrus anterior division	R	58, -2, -22	-2.56	0.015

Table 3. 6. Differences in NAc shell and core functional connectivity profiles within HC and CBP participants after correcting for multiple comparisons ($q < 0.05$).

3.4.2. NAc Connectivity Differences Between Groups

There was no significant difference between shell and core connectivity between the two groups (main effect of region, shell X core between HC and CBP on the right ($p = 0.635$) or left ($p = 0.994$) side). However, irrespective of NAc subregion, both NAc regions showed a significant difference in NAc whole brain connectivity between HC and CBP (main effect of group, HC and CBP, left ($p = 0.003$) and right ($p = 0.003$) sides). These results suggest that while shell and core connectivity profiles are similar in HC and CBP patients, overall NAc connectivity is different between groups.

The specific connections that were significantly different between HC and CBP are listed in Table 3. 7. and visualized in Figure 3. 6. A-B; based on the network each region belonged to, we determined how many significant connections there were with the shell or core and mapped them to five known RSNs (Figure 3. 6. C). While HC had more connections to the language/memory and salience networks, CBP had more connections to the default mode and attention/executive networks.

	Hemi.	**MNI coordinates (x, y, z)**	***t*-stat**	***p*-value**
HC > CBP (Left Core)				
Planum polare	L	-48, -4, -6	-4.99	< 0.001
Heschls Gyrus	L	-48, -18, 6	-4.62	< 0.001
Central Operculum	L	-48, -4, 8	-4.34	< 0.001
Intracalcarine Cortex	L	-6, -74, 12	-4.16	< 0.001
Middle Insula	L	-6, 18, 34	-3.97	< 0.001
Hippocampus	L	-28, -22, 16	-3.96	< 0.001
Lingual Gyrus	L	-10, -68, -2	-3.95	< 0.001
Superior temporal gyrus anterior division	L	-58, -4, -6	-3.95	< 0.001
Posterior Insula	L	-38, -14, 8	-3.89	< 0.001
Lingual Gyrus	R	10, -68, -2	-3.47	0.001
Intracalcarine Cortex	R	-6, -74, 12	-3.28	0.002
Parahippocampal gyrus, posterior division	L	-24, -32, -18	-3.28	0.002
Supracalcarine Cortex	L	-2, -84, 12	-3.10	0.003
Planum temporale	L	-60, -22, 8	-2.99	0.004
Temporal occipital fusiform cortex	L	-34, -54, -16	-2.87	0.005
HC > CBP (Left Shell)				
Planum polare	L	-48, -4, -6	-5.25	< 0.001
Superior temporal gyrus anterior division	L	-58, -4, -6	-4.85	< 0.001
Hippocampus	L	-28, -22, -16	-4.55	< 0.001
Central Operculum	L	-48, 4, 8	-4.35	< 0.001
Heschls Gyrus	L	-48, -18, 6	-4.33	< 0.001
Middle Insula	L	-40, -2, -2	-4.06	< 0.001
Parahippocampal gyrus, posterior division	L	-24, -32, -18	-4.02	< 0.001

	Hemi.	MNI coordinates (x, y, z)	*t*-stat	*p*-value
Lingual gyrus	L	-10, -68, -2	-3.88	< 0.001
Intracalcarine Cortex	L	-6, -74, 12	-3.76	< 0.001
Posterior Insula	L	-38, -14, 8	-3.62	0.001
Temporal occipital fusiform cortex	L	-34, -54, -16	-3.61	0.001
Lingual Gyrus	R	10, -68, -2	-3.47	0.001
Superior temporal gyrus, posterior division	L	-66, -26, 6	-3.13	0.002
Temporal Pole	L	-40, 16, -30	-3.08	0.003
Temporal occipital fusiform cortex	R	34, -54, -16	-3.01	0.004
Temporal fusiform cortex posterior division	L	-36, -16, -32	-3.00	0.004
Planum temporale	L	-60, -22, 8	-2.90	0.005
Occipital fusiform gyrus	L	-28, -76, -14	-2.81	0.006
Intracalcarine Cortex	R	6, -74, 12	-2.76	0.007
Hippocampus	R	28, -22, -16	-2.69	0.009
CBP > HC (Left Core)				
Dorsolateral prefrontal cortex	R	40, 20, 44	3.69	< 0.001
Dorsal medial prefrontal cortex anterior division	L	-4, 50, 28	3.45	0.001
Dorsolateral prefrontal cortex	L	-40, 20, 44	3.19	0.002
Dorsal medial prefrontal cortex posterior division	L	-4, 26, 48	3.01	0.003
Dorsal medial prefrontal cortex posterior division	R	4, 26, 48	2.97	0.004
Dorsal medial prefrontal cortex anterior division	R	4, 50, 28	2.84	0.006
CBP > HC (Left Shell)				
Dorsolateral prefrontal cortex	R	40, 20, 44	3.96	< 0.001
Dorsal medial prefrontal cortex anterior division	L	-4, 50, 28	3.41	0.001
Dorsolateral prefrontal cortex	L	-40, 20, 44	3.31	0.001
Dorsal medial prefrontal cortex posterior division	L	-4, 26, 48	3.24	0.002
Dorsal medial prefrontal cortex posterior division	R	4, 26, 48	3.06	0.003
Dorsal medial prefrontal cortex anterior division	R	4, 50, 28	2.92	0.005
HC > CBP (Right Shell)				
Hippocampus	L	-28, -22, -16	-3.92	< 0.001

	Hemi.	MNI coordinates (x, y, z)	*t*-stat	*p*-value
Posterior Insula	L	-38, -14, 8	-3.77	< 0.001
Central Operculum	L	-48, -4, 8	-3.45	0.001
Planum polare	L	-48, -4, -6	-3.45	0.001
Heschls Gyrus	L	-48, -18, 6	-3.45	0.001
Superior temporal gyrus anterior division	L	-58, -4, -6	-3.40	0.001

Table 3. 7. Differences in functional connectivity in the shell and core between CBP and HC subjects after correcting for multiple comparisons. No significant values were found for the right core, HC > CBP and CBP > HC, as well as for right shell, CBP > HC. Abbreviations: PIP, planum polare; STGa, superior temporal gyrus anterior division; pHippp, parahippocampal gyrus, posterior division; PIT, planum temporale; TOF, temporal occipital fusiform cortex; STGp, superior temporal gyrus, posterior division; TFCp, temporal fusiform cortex posterior division; OccFG, occipital fusiform gyrus; dlPFC, dorsolateral prefrontal cortex; dmPFCa, dorsal medial prefrontal cortex anterior division; dmPFCp, dorsal medial prefrontal cortex posterior division.

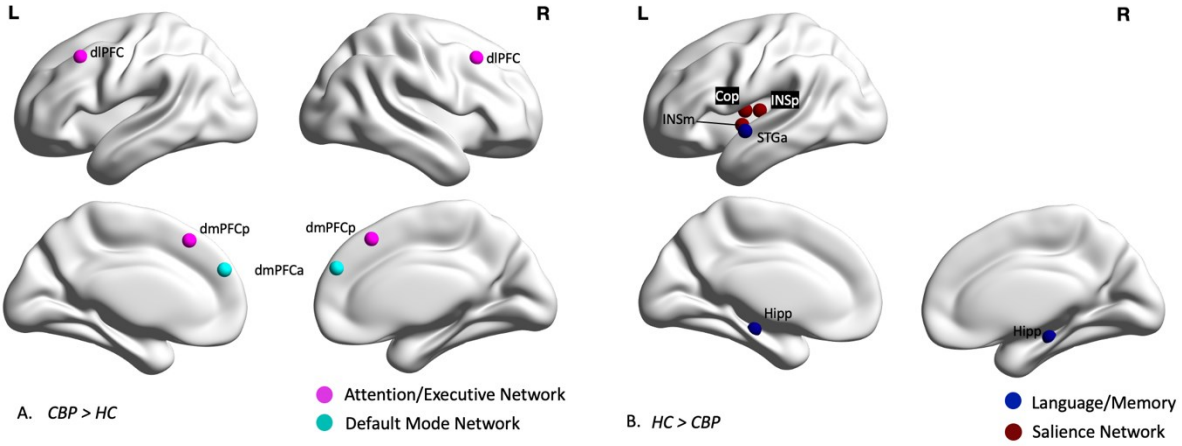

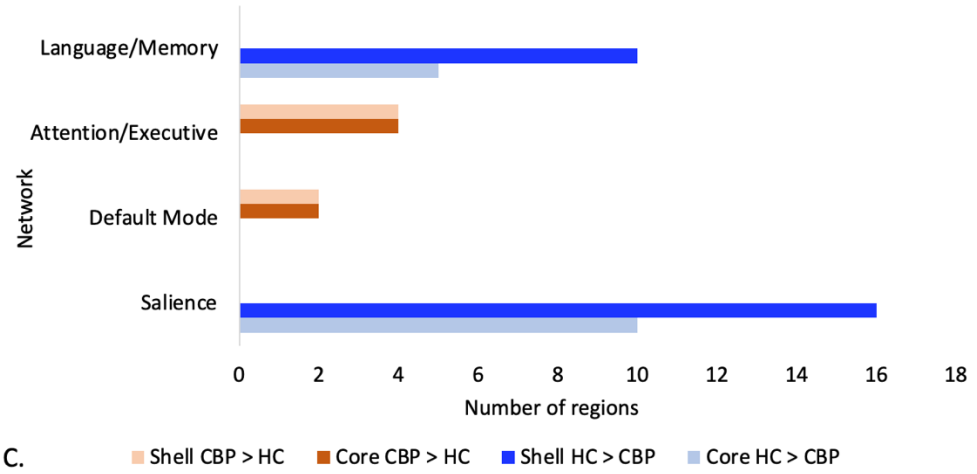

Figure 3. 6. Functional connectivity contrast analyses reveal differential connectivity between healthy controls (HC) and chronic back pain (CBP) patients in both the NAc shell and core. **A**. The significant CBP > HC contrasts; **B**. The significant HC > CBP nodes; **C.** Quantification of significant nodes in the CBP > HC and HC > CBP contrasts into their respective networks. CBP patients had more connections to the attention/executive and default mode networks, while HC had more connections to language/memory and salience networks. Note: left and right brain images represent sagittal views; the top set are viewed from the lateral side while the bottom set are viewed from the medial side at the midbrain. Whole brain corrected at $p < 0.05$. *Abbreviations:* Cop, central operculum; INSm, middle insula; INSp, posterior insula; dlPFC, dorsolateral prefrontal cortex; dmPFCa, dorsal medial prefrontal cortex anterior division; dmPFCp, dorsal medial prefrontal cortex posterior division; Hipp, hippocampus; STGa, superior temporal gyrus, anterior division.

3.4.3. Association Between the rsFC Network and Clinical Measures

Next, we wanted to find connections that were associated with chronic pain intensity. The specific edges of interest were revealed in the CBP > HC and CBP < HC contrasts. We correlated these edges with BPI and NPS pain intensity scores. There were no significant correlations between the CBP > HC and CBP < HC connections and BPI (average pain score and total areas of pain) scores (FDR $q < 0.10$). However, after FDR correction at $q < 0.10$, chronic pain intensity correlated with several NAc – prefrontal cortex connections and one NAc – temporal lobe connection (Figure 3. 7.), revealing connections that are specific to chronic pain.

Thus, in the CBP > HC contrast, the shell showed higher connectivity with regions involved in cognition such as top-down processing left shell-right dlPFC ($r = 0.32$, $p = 0.022$), left core-right dlPFC ($r = 0.37$, $p = 0.007$) and cognitive appraisal left shell-left dmPFCa ($r = 0.33$, $p = 0.018$), left shell-right dmPFCa ($r = 0.37$, $p = 0.007$), left core-left dmPFCa ($r = 0.36$, $p = 0.010$), and left core-right dmPFCa ($r = 0.43$, $p = 0.001$). Finally, in the CBP < HC contrast, chronic pain intensity was significantly negatively correlated with the left core-right temporal occipital fusiform cortex ($r = -0.50$, $p < 0.001$).

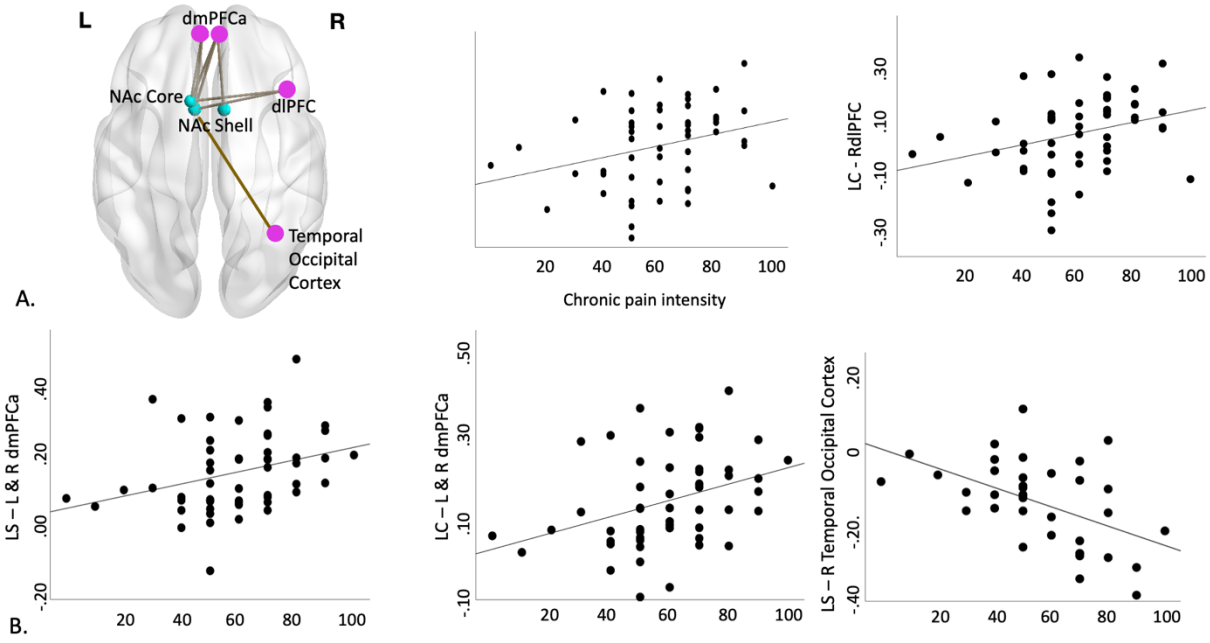

Figure 3. 7. The significant contrasts in the CBP > HC rsFC comparison were used in further analyses to determine clinical pain parameter correlations and classifications. **A**. Axial view of significant rsFC connections between the NAc shell and core and regions that were correlated to chronic pain intensity. **B**. Scatter plots of the correlations between the significant CBP > HC and CBP < HC contrasts and the pain intensity subscale of the NPS. The functional connectivity values for both the left and right side of the dmPFCa were averaged for simplification, as no significant differences were found between the left and right side (bottom two scatter plots). *Abbreviations:* NAc, nucleus accumbens; dmPFCa, dorsal medial prefrontal cortex anterior division; dlPFC; dorsolateral prefrontal

cortex; LC, left core; LS, left shell; RS, right shell; NPS, neuropathic pain scale. Correlations were FDR corrected for multiple comparisons at $p < .05$.

3.5. Reproducibility Analyses

To gain confidence in the findings of the clinically relevant NAc edges, we analyzed whether these connections were reproducible in within sample and out of sample data, and whether these edges could accurately classify between CBP and HC groups (Figure 3. 8.).

To this end, the area under the ROC curve was calculated in the initial combined rest 1 and 2 dataset (Figure 3. 8. A-B). The rsFC values between the left shell-right dlPFC, the left core-right dlPFC, left shell-left dmPFCa, left core-left dmPFCa, and left core-right temporal occipital fusiform cortex were moderate predictors of classifying between HC and CBP groups (AUC $\geq$ 0.7; panel B).

We then separated rest 1 and 2 (Figure 3. 8. C and D) to test whether the two resting state scans mediated the significant differences between groups. Both rest one and two showed similar differences in rsFC values, pointing to reproducible within-subject effects during two separate scans.

We then tested these whether these connections reproduced in an out of sample validation dataset (Figure 3. 8. E). Only the left shell and core connection to the right dlPFC reproduced in the validation dataset.

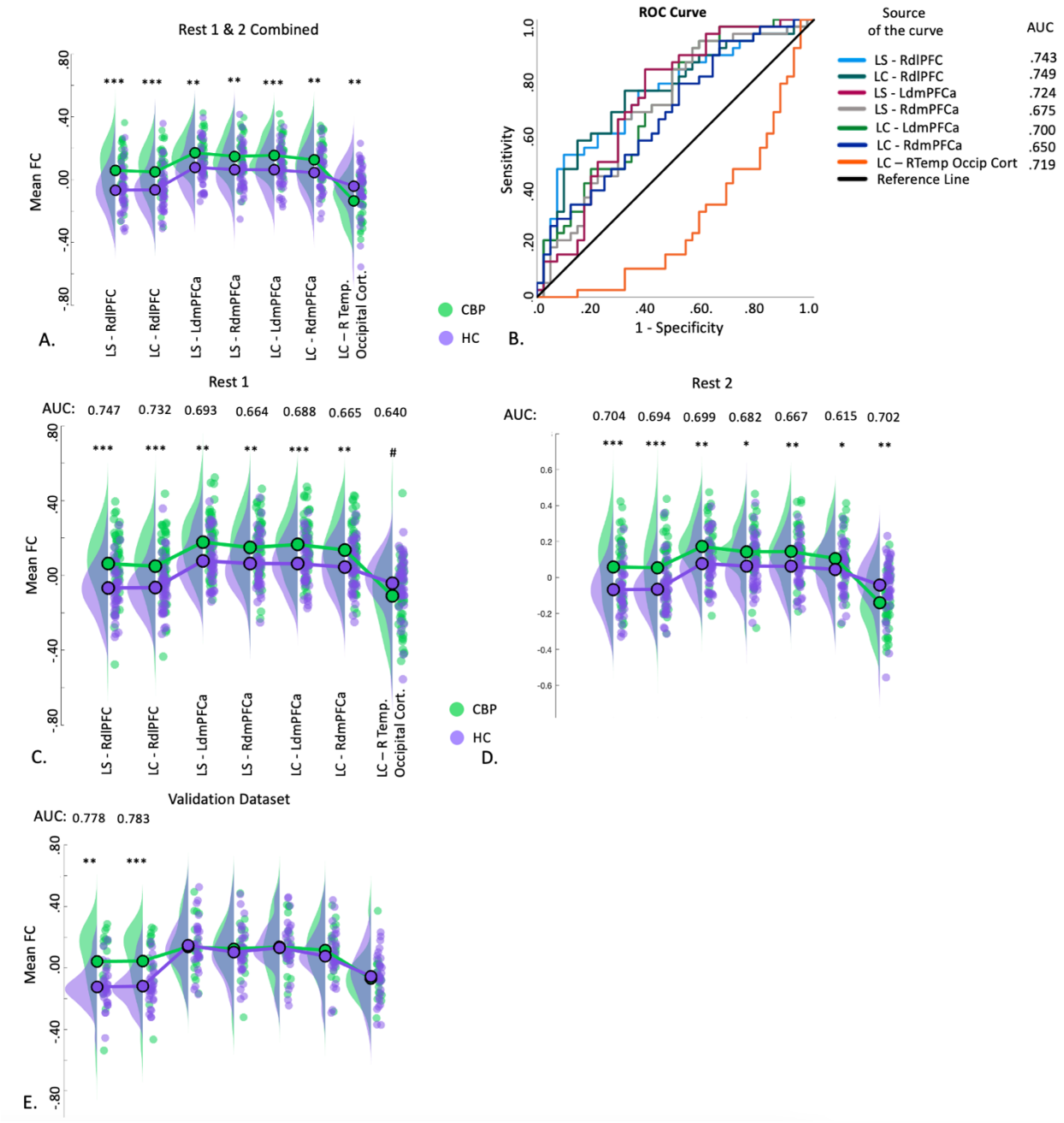

Figure 3. 8. The connections that were significantly correlated with chronic pain intensity were assessed for their ability to accurately classify between groups in the initial dataset, the two separate resting state scans taken in the CBP group from the initial dataset, and the two validation datasets. **A.** The initial combined rest 1 and rest 2 group consisted of $n = 39$ CBP patients and $n = 41$ HC; HC data were taken from a single resting state scan for all three initial comparisons (panel A., C., and D.). **B.** The receiver operator characteristic (ROC) curves revealed five out of seven connections to be moderate predictors (AUC > 0.7) of classifying between HC and CBP. **C.** Comparison of

connections in rest 1 (n = 54 CBP) and the associated AUC values. **D.** Comparison of CBP and HC in rest 2 (n = 42 CBP) and associated AUC values. Both rest 1 and rest 2 revealed reproducible results, confirming within-subjects reproducibility across scans. **E.** Comparison of groups in a validation dataset (n = 18 CBP and 30 HC) revealed significant differences between groups in the left shell and core to the right dorsolateral PFC. These results point to the rdlPFC as an especially important region that can distinguish CBP from HC. *Abbreviations:* AUC, area under ROC; dlPFC, dorsolateral prefrontal cortex; dmPFCa, dorsal medial prefrontal cortex anterior division; LC, left core; LS, left shell; ROC, receiver operator characteristic; RS, right shell. *Significances:* #, $p = 0.05$, * $p < 0.05$, ** $p < 0.01$, *** $p < 0.001$.

CHAPTER 4. Discussion

4.1. Summary of Key Findings

The results of this thesis describe how pain perception is altered by both bottom-up stimulus characteristics and top-down expectation effects, how these two factors map onto NAc activation, and how intrinsic NAc shell and core connectivity is different between healthy individuals and those with chronic pain. The ability to determine how the NAc and other important neural regions respond to pain and are altered during pain chronification can provide greater insight into more targeted therapies to manage pain.

The first objective was to understand the behavioural response to static vs. dynamic stimuli and characterize expectation effects in these different stimulus types. In line with previous studies (Atlas et al., 2010; Lim et al., 2020; Shih et al., 2019) the behavioural results show that threat predictions influence pain perception. Extending these findings, expectation effects from static stimuli were greater than those from dynamic stimuli.

The next objective was to determine how the NAc, an important pain and expectation processing region, behaves in response to different combinations of stimulus characteristics and expectation effects. The NAc was an important region for responding to and evaluating cued threats, with differential activation depending on the perceived threat and stimuli type. When investigating NAc subregions, while both the core and shell were involved in evaluating painful stimuli, the core was better able to discriminate between conditions during heat stimuli relative to the shell, activating more during uncued and positive expectation conditions. Overall, this is the first study to compare static and dynamic stimuli behaviourally, via a threat prediction paradigm; and neurologically, via whole-region and subregion NAc activation analyses.

Finally, the last objective sought to characterize differences in core and shell connectivity within and between HC and CBP patients by analyzing differences during resting state. As well,

significant connections in the CBP > HC and CBP < HC contrasts were used to identify clinically relevant CBP networks and were assessed based on their reproducibility. Patients with CBP were found to have hypoconnectivity to the salience and language/memory networks and hyperconnectivity to the default mode and attention/executive networks, specifically regions in the dorsomedial and dorsolateral PFC, relative to HC. As well, reproducibility analyses revealed the NAc connection to the right dlPFC to be a particular region of interest that can reliably distinguish between HC and CBP patients. These findings support the idea that frontal-subcortical connectivity patterns crucial for the generation and regulation of emotion are altered in CBP patients relative to HC.

4.2. Expectation and Stimuli Characteristic Effect Pain Perception

The presence of cues was sufficient to alter pain perception; this is in line with similar work showing that pain ratings were more aligned with cued threat values relative to purely bottom-up sensory feedback during uncued epochs (Lim et al., 2020).

Positive expectation reduced pain perception while negative expectation did not increase pain perception, and static stimuli biased pain perception more than the dynamic stimuli. This is in line with previous work implicating expectations in altering pain perception during both simple, Pavlovian conditioning (Atlas et al., 2010) and more complex, schema-driven conditioning (Lim et al., 2020). While negative expectations are undoubtedly prevalent in a variety of settings (Colloca & Barsky, 2020), the temperature may have been too low to significantly influence pain perception during the negative expectation condition, causing participants to rate their pain on the low end of the rating scale and introducing a floor effect. Indeed, many participants rated their pain near 0 on the NRS.

In line with the hypothesis, static stimuli produced more of an expectation effect relative to dynamic stimuli, suggesting that participants were more vigilant to the bottom-up properties and less so to the top-down cueing effects in dynamic relative to static stimuli. Indeed, Hashmi and Davis (2008) showed that the temporal profile of sharp, stinging, and cutting qualities induced at stimulus onset receded during static, but not dynamic, stimuli. Since threat systems have evolved to detect changing threats (Croze, Duclaux, & Kenshalo, 1976), and adaptation to pain may primarily involve C-fibers (Tracey, 2017), it is likely that the static, but not dynamic, stimuli in our study involved a greater degree of adaptation. Therefore, participants experiencing static stimuli could be more suggestible to top-down cuing effects due to rapid adaptation that occurs in static relative to dynamic stimuli (where the bottom-up circuits maintain vigilance to the pain experienced).

4.3. Nucleus Accumbens Task Activation

Previously, the NAc has been shown to activate during anticipating reward in humans (Knutson et al., 2008). Conversely, the thesis results show no difference in whole or subregion NAc activation during the anticipation of different levels of pain. This may be due to the NAc as a neural marker of positive arousal, and other regions (e.g., the insula) as a marker for negative arousal. In a study of monetary gains and losses, the NAc activation increased in anticipation for monetary gains but decreased in anticipation of losses (Cooper & Knutson, 2008).

During heat, there was greater differentiation in NAc activation for dynamic stimuli versus static stimuli between conditions. Since the NAc is a region that detects the motivational salience of stimuli (Ventura, Morrone, & Puglisi-Allegra, 2007), the non-changing nature of static stimuli may not have been salient enough to provoke differential activation of the NAc between the uncued, matched, and positive expectation during heat, even during high

temperatures. Conversely, dynamic stimuli have more motivational salience due to their changing and unpredictable nature, evoking a more graded NAc response between the uncued and positive expectation condition relative to the matched expectation condition. Additionally, despite static and dynamic stimuli reaching the same peak temperature (47°C), participants rated the dynamic stimuli as more painful, and therefore more motivationally salient, compared to the static stimuli. Given that the NAc engages in events that involve dynamic alterations in the relation between probability of reward and decisions (Nachev et al., 2015), the NAc may be primed to respond to stimuli that are unpredictable, or dynamic, in nature. While there was an increase in general activation in the NAc to the static stimuli, the NAc did not differentiate between expectation conditions. This suggests that the NAc did not perceive the static conditions as motivationally salient and that the NAc responds to stimuli that are less predictable and changing in nature.

Both the core and shell seem to be involved during rating events, with the unknown condition elucidating the most NAc inactivity. Surprisingly, rating effects were only present during static, but not dynamic, stimuli. This may be because static stimuli produced greater expectation effects relative to dynamic stimuli, so while NAc activity did not differ during heat, there was greater discrimination in NAc activity during the rating period in static stimuli as participants tried to evaluate their pain.

Furthermore, the NAc core was important in responding to both uncertain threats and violations in cue-stimuli associations (prediction errors). The NAc core did not seem to mediate the top-down effect of expectations on pain, instead, it encoded the prediction error between expected and actual noxious events, specifically for dynamic stimuli. Previous work showed that NAc dopamine receptors in the core, but not shell, play a role in fear prediction error in rats (S.

S. Li & McNally, 2015), and that core dopamine release encodes both positive and negative reward prediction errors (Hart et al., 2014). These studies support the prevailing theory of reward prediction error, which states that dopamine signaling updates associations between rewards and predictive cues by encoding perceived errors between predictions and outcomes (Schultz, Dayan, & Montague, 1997). This theory is limited in that it cannot describe other dopamine-related phenomena, such as behaviour driven by aversive stimuli. While the NAc has not been viewed as a central hub in the threat network, there is a growing body of literature implicating the NAc, especially the core, in threat processes (Wenzel, Rauscher, Cheer, & Oleson, 2015; Zhang et al., 2020). However, reports, especially from single-cell recordings, have been conflicting. Several studies suggest that NAc dopaminergic neurons are inhibited by aversive stimuli, while others find no change or even an increase in neural activity (Wenzel et al., 2015).

In humans, the whole NAc was found to activate similarly during both conditioned appetitive and aversive stimuli, suggesting attention is guided more by motivational salience and less by separate systems for positive and negative stimuli (Kim et al., 2021). Indeed, this is in line with evidence of NAc recruitment in valence-independent signals like surprise (Shulman et al., 2009). In animals, recent developments suggest that the NAc core signals the perceived salience of stimuli during aversive events (Kutlu et al., 2021). As well, most NAc core neurons showed the greatest firing change in response to danger and uncertainty (M. H. Ray et al., 2022). Overall, these findings imply a role of the NAc core in encoding perceived salience signals independent of valence.

Nucleus accumbens core activity seemed to act in line with these recent findings, where the increased perceived salience during heat in uncertain and positive expectation conditions resulted in increased activation of the NAc core relative to the matched or negative expectation

conditions. In the current results, this was only apparent in the dynamic, but not static, stimuli, potentially due to the NAc's role in responding to dynamic alterations in reward processes (Nachev et al., 2015) and the unpredictable nature and increased perceived pain that dynamic stimuli provoked in participants. Thus, the NAc core seems to be encoding the perceived salience of threatening stimuli, which is sensitive to bottom-up properties of the stimulus.

4.4. Nucleus Accumbens Activity is Associated with Affective Measures

Finally, during the evaluation of painful stimuli, there were positive associations between measures of mindfulness and NAc activity during positive expectation and negative correlations with measures of depression and anxiety. However, during negative expectation, the association switched: mindfulness was negatively correlated, and depression and anxiety were positively associated with NAc activity. Previously, there have been reports of increased NAc activation during ecstatic meditation (Hagerty et al., 2013) and dampened activity during stress and depression (Pittenger & Duman, 2008).

As well, NAc activation was positively correlated with depression and anxiety scores during heat in the static condition, but not in the dynamic condition, suggesting that individuals use more subjective evaluation during static heat and this subjectivity is driven in part by their affective state. In animals, dopamine levels increased in response to stress (Kalivas & Duffy, 1995), and repeated stress alters signalling to the NAc and leads to depressive symptomology (Francis & Lobo, 2017).

4.5. Nucleus Accumbens Core and Shell Exhibit Similar Intrinsic Connectivity

The current thesis supports the framework that the NAc core is responsible for driving the response to uncertain threats and to painful dynamic expectation effects. From previous research, NAc activity has been intimately involved in the pain response (Fields, 2018). Since CBP

patients often have a history of expected treatment failure and a high degree of uncertainty regarding their condition (Moulin et al., 2002; Simon, 2012), characterizing the connectivity differences in the NAc core and shell between those with CBP and those without was of particular interest.

When analyzed separately, similar patterns of shell and core rsFC were found in both HC and CBP participants: whereas the core preferentially connected to subcortical and salience networks, the shell preferentially connected to language/memory and default mode networks. This result suggests distinct functionality between the shell and core, irrespective of chronic pain, and extends previous findings of dissociable shell and core connectivity. To our knowledge, no other study has thoroughly characterized which regions the core preferentially connects to over the shell and vice-versa using rsFC in humans. Previous findings, mainly conducted in non-human animals, show prominent core connections with the orbitofrontal cortex, anterior cingulate cortex, amygdala, thalamus, substantia nigra, and "basal ganglia-like" subcortical structures (Daniel S Zahm, 2000). On the other hand, the shell has prominent connections with the medial prefrontal cortex, hippocampus, amygdala, ventral pallidum, and periaqueductal grey (Daniel S Zahm, 2000).

Given that one of the main roles of the shell is to the assign subjective values to competing stimuli (Seeley, 2019), its preferential connections to DMN regions that play a role in value judgements (e.g., PFC) supports this general function. While the shell seems to be involved with flexibly tracking the motivational value of rewards (Chaudhri, Sahuque, Schairer, & Janak, 2010; Loriaux, Roitman, & Roitman, 2011), it is also involved in aversive learning: for example, it was found to be active during fear extinction (Dutta, Beaver, Halcomb, & Jasnow, 2021). The thesis results also support the current literature of shell projections to the PFC and ventral

tegmental area (VTA), which send dopaminergic projections to mesocortical sites (Groenewegen, Berendse, & Haber, 1993; Heimer et al., 1991). Efferents of the shell also include hubs of the DMN, such as the mPFC (Salgado & Kaplitt, 2015); these pathways are important for cognitive control, motivation, and learning (Hauser, Eldar, & Dolan, 2017). The DMN, a group of regions generally associated with functions such as spontaneous cognition and mind-wandering (Christoff, Gordon, Smallwood, Smith, & Schooler, 2009; Mason et al., 2007), deserves special attention due to its multifaceted role in functions as diverse as creativity, goal-directed tasks, and future thinking (Spreng, Mar, & Kim, 2009; Sunavsky & Poppenk, 2020). Functionally, the shell is thought to be involved with encoding the hedonic value of stimuli and suppressing less- or non-rewarding stimuli that may interfere with the best available choice (Stopper & Floresco, 2011; West & Carelli, 2016). These processes involve DMN regions linked to the high-level cognitive aspects of cognitive control (e.g., mPFC) (Spreng, Stevens, Chamberlain, Gilmore, & Schacter, 2010) and memory regions linked to learning processes (e.g., parahippocampus) (Okano, Hirano, & Balaban, 2000).

The core, on the other hand, is thought to be involved in instigating an approach to the most appropriate stimuli, as such, core connectivity to motor regions (e.g., supplementary motor area) supports this idea. The core is also important for cue-induced reward seeking and addictive behaviours and has bidirectional control over both appetitive and aversive responses as well as fear expression (Chaudhri et al., 2010; Dutta et al., 2021; Hamel, Thangarasa, Samadi, & Ito, 2017). Core connectivity to salience (e.g., anterior cingulate and frontoinsular regions) and subcortical (e.g., caudate, putamen) networks support the relevance of this region in perceiving, processing, planning, and responding via action pathways to motivationally salient stimuli (Seeley, 2019). For example, core neurons were found to signal valence in response to cues,

increasing firing in anticipation of rewards and decreasing firing in anticipation of threats or uncertain cues (Madelyn H. Ray, Moaddab, & McDannald, 2021). The preferential NAc core connections to salience regions found in our study may be involved with this detection and perception process (Seeley, 2019). The preferential core connections to the subcortical network, meanwhile, eventually lead to the premotor and supplementary motor areas (Salgado & Kaplitt, 2015; D. S. Zahm, Williams, & Wohltmann, 1996), suggesting that the core may be important in planning the execution of motivationally driven movements (Salgado & Kaplitt, 2015).

4.6. Network-level Core and Shell Connectivity Differences Between Groups

This thesis demonstrates that people with chronic back pain show reproducible hyperconnectivity between accumbens and prefrontal cortices. This hyperconnectivity predicts chronic pain intensity. In line with recent discoveries implicating connectivity between the NAc and regions within the prefrontal cortex in CP (Makary et al., 2020), our results extend the current literature by finding clinically relevant NAc – PFC connections that distinguish HC from CBP.

The data-driven connectomics approach used identified medial and lateral PFC regions as hyperconnected to NAc in people with CBP relative to healthy controls; higher connectivity was also predictive of chronic pain intensity. Nucleus accumbens connectivity with PFC has been implicated widely in animal studies and in vivo in humans. Lee et al. (2015) showed that optogenetic activation of the PFC produces pain-relieving responses in a rat model of neuropathic pain; the authors of that study concluded that this function of the PFC was likely mediated by the NAc. In rodents, NAc – PFC circuits showed increased sensitization in neuropathic states and this changed behavioral responses to morphine reward (Kai et al., 2018). Similarly, inhibiting PFC activity or its projections to the NAc increased rodent sensitivity to

sensory and affective stimuli (Zhou et al., 2018). The authors concluded that PFC projections to the NAc are important for pain regulation and alterations contribute to the aetiology of chronic pain.

In humans, increased NAc – mPFC/ACC functional connectivity has been linked to the transition from acute to CP, and this connection was a dominant predictor of persistence of pain in a longitudinal study (M. N. Baliki et al., 2012). With a stringent voxel wise seed based rsFC technique, Makary and colleagues (2020) observed increased connectivity from the NAc shell and core to the right ACC that covaried with back pain intensity, but only during the earlier stages of chronic pain development. They did not find any differences in NAc connectivity between HC and CBP patients after correcting for multiple comparisons. The duration for CBP was longer in this thesis (7.5 years in the initial dataset and 5.8 years in the validation dataset). Another study also looking at the transition from acute to early stages of CBP (approximately 1 year) (Vachon-Presseau et al., 2016) revealed that while those with persistent back pain had a higher incidence of functional connections within a dmPFC-amygdala-NAc module relative to those with acute back pain, this group difference did not persist at follow-up three years later. This variability circles back to different resolution data, preprocessing techniques, CBP duration and study objectives. The systematic analysis in this thesis demonstrate that NAc-PFC connectivity can indeed be reliably and reproducibly observed in higher resolution data. The NAc was hyperconnected with several nodes within the default mode network and the attention/executive networks and hypoconnected with sensory and language memory networks. Another study looking at functional differences across RSN's between CBP patients and HC found decreased mPFC and increased precuneus representation within the DMN in CBP patients relative to HC, suggesting that CP may alter DMN function by altering higher cognitive

processes (Marwan N Baliki, Mansour, Baria, & Apkarian, 2014). The thesis findings, while somewhat divergent, consistently underscore the significance of NAc – PFC connectivity in the aetiology of chronic pain.

The PFC is a multimodal region important for higher order cognitive processes related to thinking, planning, and acting to enhance survival. For instance, the PFC is associated with cognitive processing (e.g., dlPFC) (Koyama, O'Connor, Shehzad, & Milham, 2017) and generating and regulating emotion (e.g. dmPFC) (Etkin, Buchel, & Gross, 2015). The dmPFC in particular is a component of the DMN and a functionally heterogenous region generally associated with attention (Vossel, Geng, & Fink, 2014), value encoding (Sokol-Hessner, Hutcherson, Hare, & Rangel, 2012), creativity (Liu et al., 2015), decision making (Philiastides, Auksztulewicz, Heekeren, & Blankenburg, 2011), emotion regulation (Etkin et al., 2015) processes and relatedly, in cognitive appraisals of pain (O'Reilly, 2010; Wei et al., 2016). The high NAc – PFC connectivity observed in several studies is indicative of synchronisations between reward processing and higher-order processes related to working memory, attention and self-referential thinking/planning in chronic pain. For instance, PFC activity increases in both positive and negative emotion-induction tasks, often in concert with subcortical activation such as through ventrolateral PFC – NAc connections (Kober et al., 2008; Wager, Davidson, Hughes, Lindquist, & Ochsner, 2008); this pathway may be important for exerting the effects of chronic pain related priors such as rumination and fear. The variability in identified PFC regions highlights the divergent yet overlapping functions of different parts of the PFC complex. This region is markedly more expanded in humans and the modules with specific higher order functions need to be explored for their specific roles in pain learning processes. For instance, the dlPFC is involved in pain modulation (Lorenz, Minoshima, & Casey, 2003), has been shown to

have abnormally increased function in CP populations, and is involved in downregulating pain-evoked activation in important pain-processing regions when pain is controllable (Brascher, Becker, Hoeppli, & Schweinhardt, 2016). Non-invasive stimulation of the dlPFC is being purported to reduce CP symptoms (Seminowicz & Moayedi, 2017). A recent meta-analysis (Che et al., 2021) found that repetitive Transcranial Magnetic Stimulation induced an analgesic effect in CP and in response to provoked pain. Thus, our study partially supports these previous observations and extends them by specifically pointing to NAc connectivity with the dlPFC as a key feature that can distinguish between CBP and HC. In contrast, the dmPFC is a key component of the dorsal sub-network within the DMN and plays an important role in emotional appraisal (Etkin et al., 2015) and is implicated in CBP development (Vachon-Presseau et al., 2016). Contrasting findings from a series of findings from the same data resource have implicated the mPFC proper extending into Brodmann area 32 of the ACC in mediating spontaneously increases in CBP intensity (M. N. Baliki et al., 2012; Hashmi et al., 2013). Taken together, these findings indicate that PFC sub-regions underpin different stages of CBP pathophysiology and the connectivity with NAc points towards a synchronized role of NAc and PFC in maladaptive top-down processing in people with CBP.

Additionally, hyperconnectivity between NAc – dmPFC may alter normal top-down regulation processing and may contribute to feelings of pain in CBP if bottom-up signals are ignored, partly or completely. In fact, PFC activity increases in both positive and negative emotion-induction tasks, often in concert with subcortical activation such as through ventrolateral PFC – NAc connections (Kober et al., 2008; Wager et al., 2008); this pathway may be important for exerting the effects of negative expectations on pain processing. Broad functional changes within DMN and striatal regions are well documented in depression and

anxiety (Disner, Beevers, Haigh, & Beck, 2011); the altered connectivity seen in our results is consistent with the high prevalence of co-morbid depression and anxiety disorders in CBP populations (Demyttenaere et al., 2007), as well as the higher BDI scores from CBP patients in this thesis. Conversely, CBP patients showed reduced NAc connectivity to salience regions such as the posterior insula, which is involved in intensity encoding, localization, learning, and memory of noxious stimuli (Segerdahl, Mezue, Okell, Farrar, & Tracey, 2015). These connectivity patterns may be needed for normal integration of bottom-up stimuli in regions within the insula and ACC with top-down modulatory regions such as the dmPFC.

Interestingly, contrary to previous findings implicating chronic pain changes mainly to frontal regions, here we show that more posterior regions are involved in CBP, like the temporal occipital fusiform cortex. While this connection was not reproduced in a separate dataset, it was negatively associates with pain intensity and was an accurate classifier between HC and CBP patients. Recently, (Mayr et al., 2022) found that areas in the occipital fusiform gyrus and temporal fusiform gyrus to be important in encoding changes in pain intensity in CBP patients. Additionally, reduction of cortical thickness in the temporal gyrus in CP patients in a 7-year longitudinal study was found relative to HC (Muthulingam et al., 2018). More research should focus on elucidating the NAc connections with temporal, parietal, and occipital regions in CP populations.

4.7. Limitations and Future Directions

A limitation to study one is our inability to directly compare absolute pain values and accumbens activation between static and dynamic stimuli due to the significantly different pain ratings the participants gave during high temperatures between static and dynamic stimuli. While the peak temperature was constant across both static and dynamic high temperature stimuli, the

dynamic stimuli produced significantly higher pain ratings. Further research should focus on utilizing dynamic stimuli that produces similar pain ratings to the static stimuli to be able to compare similarly perceived levels of pain across static and dynamic stimuli and the NAc activations therein.

Finally, there was no significant negative expectation effect recorded, most likely due to a floor effect of participants rating both static and dynamic low temperature stimuli close to 0 on the NRS. While negative expectations are regularly observed in the literature (Shih et al., 2019), our temperature plateau most likely needed to be higher to observe this effect. Future work should look at pain perception and NAc core and shell activations with significant negative expectation effects as well.

A limitation to study two is the cross-sectional nature of our analyses in comparing differences between HC and CBP patients. Following participants longitudinally and tracking the progression of pain could help further elucidate functional changes in NAc connectivity. Additionally, studying how pain progresses from the acute to chronic phase with a focus on the NAc could provide better insight into the changes that are apparent in a CBP population. The main limitation is that our smoothing procedures would result in a lower spatial resolution in the shell and core, which share the same border and encompass small volumes. However, no differences in our main findings on connectivity between groups were found after running the preprocessing without the 6mm spatial smoothing kernel. As well, our protocol used multibanding with a sampling rate/voxel size balance that increases temporal resolution without negatively impacting the signal to noise ratio and has been used in our previous studies on small brainstem structures see (Wang et al., 2022).

Finally, most participants were female in the CBP population, further research should balance sex within CP groups and compare between sexes for differences with even larger datasets. Future work should also be aimed at investigating the connections between NAc and different PFC regions within the scope of their functional behavioral roles in mediating CBP aetiology.

4.8. Conclusions

There is incredible individual variation in pain perception, and the neural changes that underlie chronic pain remain a rich topic of study. Pain perception is also clearly influenced by the nature of the incoming stimuli and expectation of pain, with discernible differences in NAc activation accompanying them. The NAc core and shell are connected differently with other regions during rest in healthy individuals versus those with CBP. As opposed to other studies mainly linking aberrant NAc–mPFC connectivity in CBP, this thesis points to a more nuanced picture involving a subset of PFC connections.

References

Almeida, T. F., Roizenblatt, S., & Tufik, S. (2004). Afferent pain pathways: a neuroanatomical review. *Brain Res, 1000*(1-2), 40-56. doi:10.1016/j.brainres.2003.10.073

Andrew, D., & Greenspan, J. D. (1999). Peripheral coding of tonic mechanical cutaneous pain: comparison of nociceptor activity in rat and human psychophysics. *J Neurophysiol, 82*(5), 2641-2648. doi:10.1152/jn.1999.82.5.2641

Apkarian, A. V., & Hodge, C. J. (1989). Primate spinothalamic pathways: II. The cells of origin of the dorsolateral and ventral spinothalamic pathways. *J Comp Neurol, 288*(3), 474-492. doi:10.1002/cne.902880308

Atlas, L. Y., Bolger, N., Lindquist, M. A., & Wager, T. D. (2010). Brain mediators of predictive cue effects on perceived pain. *J Neurosci, 30*(39), 12964-12977. doi:10.1523/JNEUROSCI.0057-10.2010

Badrinarayan, A., Wescott, S. A., Vander Weele, C. M., Saunders, B. T., Couturier, B. E., Maren, S., & Aragona, B. J. (2012). Aversive stimuli differentially modulate real-time dopamine transmission dynamics within the nucleus accumbens core and shell. *Journal of Neuroscience, 32*(45), 15779-15790.

Baer, R. A., Smith, G. T., Hopkins, J., Krietemeyer, J., & Toney, L. (2006). Using self-report assessment methods to explore facets of mindfulness. *Assessment, 13*(1), 27-45. doi:10.1177/1073191105283504

Baliki, M. N., Mansour, A., Baria, A. T., Huang, L., Berger, S. E., Fields, H. L., & Apkarian, A. V. (2013). Parceling human accumbens into putative core and shell dissociates encoding of values for reward and pain. *J Neurosci, 33*(41), 16383-16393. doi:10.1523/JNEUROSCI.1731-13.2013

Baliki, M. N., Mansour, A. R., Baria, A. T., & Apkarian, A. V. (2014). Functional reorganization of the default mode network across chronic pain conditions. *PLoS One, 9*(9), e106133.

Baliki, M. N., Petre, B., Torbey, S., Herrmann, K. M., Huang, L., Schnitzer, T. J., . . . Apkarian, A. V. (2012). Corticostriatal functional connectivity predicts transition to chronic back pain. *Nat Neurosci, 15*(8), 1117-1119. doi:10.1038/nn.3153

Bardo, M., & Hammer Jr, R. (1991). Autoradiographic localization of dopamine D1 and D2 receptors in rat nucleus accumbens: resistance to differential rearing conditions. *Neuroscience, 45*(2), 281-290.

Beck, A. T., Steer, R. A., Ball, R., & Ranieri, W. (1996). Comparison of Beck Depression Inventories -IA and -II in psychiatric outpatients. *J Pers Assess, 67*(3), 588-597. doi:10.1207/s15327752jpa6703_13

Beissner, F., Brandau, A., Henke, C., Felden, L., Baumgartner, U., Treede, R. D., . . . Lotsch, J. (2010). Quick discrimination of A(delta) and C fiber mediated pain based on three verbal descriptors. *PLoS One, 5*(9), e12944. doi:10.1371/journal.pone.0012944

Berlanga, M. L., Olsen, C. M., Chen, V., Ikegami, A., Herring, B. E., Duvauchelle, C. L., & Alcantara, A. A. (2003). Cholinergic interneurons of the nucleus accumbens and dorsal striatum are activated by the self-administration of cocaine. *Neuroscience, 120*(4), 1149-1156. doi:10.1016/s0306-4522(03)00378-6

Berns, G. S., McClure, S. M., Pagnoni, G., & Montague, P. R. (2001). Predictability modulates human brain response to reward. *J Neurosci, 21*(8), 2793-2798. Retrieved from https://www.ncbi.nlm.nih.gov/pubmed/11306631

Bessou, P., & Perl, E. (1969). Response of cutaneous sensory units with unmyelinated fibers to noxious stimuli. *Journal of neurophysiology, 32*(6), 1025-1043.

Biswal, B. B., Mennes, M., Zuo, X. N., Gohel, S., Kelly, C., Smith, S. M., . . . Milham, M. P. (2010). Toward discovery science of human brain function. *Proc Natl Acad Sci U S A, 107*(10), 4734-4739. doi:10.1073/pnas.0911855107

Brascher, A. K., Becker, S., Hoeppli, M. E., & Schweinhardt, P. (2016). Different Brain Circuitries Mediating Controllable and Uncontrollable Pain. *J Neurosci, 36*(18), 5013-5025. doi:10.1523/JNEUROSCI.1954-15.2016

Burgess, P. R., & Perl, E. (1967). Myelinated afferent fibres responding specifically to noxious stimulation of the skin. *The Journal of physiology, 190*(3), 541-562.

Cartmell, S. C., Tian, Q., Thio, B. J., Leuze, C., Ye, L., Williams, N. R., . . . Halpern, C. H. (2019). Multimodal characterization of the human nucleus accumbens. *Neuroimage, 198*, 137-149. doi:10.1016/j.neuroimage.2019.05.019

Castro, D. C., & Bruchas, M. R. (2019). A motivational and neuropeptidergic hub: anatomical and functional diversity within the nucleus accumbens shell. *Neuron, 102*(3), 529-552.

Charpentier, C. J., Aylward, J., Roiser, J. P., & Robinson, O. J. (2017). Enhanced risk aversion, but not loss aversion, in unmedicated pathological anxiety. *Biological psychiatry, 81*(12), 1014-1022.

Chaudhri, N., Sahuque, L. L., Schairer, W. W., & Janak, P. H. (2010). Separable roles of the nucleus accumbens core and shell in context- and cue-induced alcohol-seeking. *Neuropsychopharmacology, 35*(3), 783-791. doi:10.1038/npp.2009.187

Che, X., Cash, R. F. H., Luo, X., Luo, H., Lu, X., Xu, F., . . . Fitzgibbon, B. M. (2021). High-frequency rTMS over the dorsolateral prefrontal cortex on chronic and provoked pain: A systematic review and meta-analysis. *Brain Stimul, 14*(5), 1135-1146. doi:10.1016/j.brs.2021.07.004

Chen, G., Adleman, N. E., Saad, Z. S., Leibenluft, E., & Cox, R. W. (2014). Applications of multivariate modeling to neuroimaging group analysis: a comprehensive alternative to univariate general linear model. *Neuroimage, 99*, 571-588. doi:10.1016/j.neuroimage.2014.06.027

Christoff, K., Gordon, A. M., Smallwood, J., Smith, R., & Schooler, J. W. (2009). Experience sampling during fMRI reveals default network and executive system contributions to mind wandering. *Proc Natl Acad Sci U S A, 106*(21), 8719-8724. doi:10.1073/pnas.0900234106

Cleeland, C. (1989). Measurement of pain by subjective report. *Advances in pain research and therapy, 12*, 391-403.

Colloca, L., & Barsky, A. J. (2020). Placebo and Nocebo Effects. *N Engl J Med, 382*(6), 554-561. doi:10.1056/NEJMra1907805

Cooper, J. C., & Knutson, B. (2008). Valence and salience contribute to nucleus accumbens activation. *Neuroimage, 39*(1), 538-547.

Cox, R. W. (2012). AFNI: what a long strange trip it's been. *Neuroimage, 62*(2), 743-747. doi:10.1016/j.neuroimage.2011.08.056

Croze, S., Duclaux, R., & Kenshalo, D. R. (1976). The thermal sensitivity of the polymodal nociceptors in the monkey. *J Physiol, 263*(3), 539-562. doi:10.1113/jphysiol.1976.sp011644

Dallenbach, K. M. (1939). Pain: history and present status. *The American Journal of Psychology, 52*(3), 331-347.

Daranyi, V., Hermann, P., Homolya, I., Vidnyanszky, Z., & Nagy, Z. (2021). An empirical investigation of the benefit of increasing the temporal resolution of task-evoked fMRI data with multi-band imaging. *MAGMA, 34*(5), 667-676. doi:10.1007/s10334-021-00918-z

Davis, K. D., & Moayedi, M. (2013). Central mechanisms of pain revealed through functional and structural MRI. *J Neuroimmune Pharmacol, 8*(3), 518-534. doi:10.1007/s11481-012-9386-8

Demyttenaere, K., Bruffaerts, R., Lee, S., Posada-Villa, J., Kovess, V., Angermeyer, M. C., . . . Von Korff, M. (2007). Mental disorders among persons with chronic back or neck pain: results from the World Mental Health Surveys. *Pain, 129*(3), 332-342. doi:10.1016/j.pain.2007.01.022

Disner, S. G., Beevers, C. G., Haigh, E. A., & Beck, A. T. (2011). Neural mechanisms of the cognitive model of depression. *Nat Rev Neurosci, 12*(8), 467-477. doi:10.1038/nrn3027

Djouhri, L. (2016). Adelta-fiber low threshold mechanoreceptors innervating mammalian hairy skin: A review of their receptive, electrophysiological and cytochemical properties in relation to Adelta-fiber high threshold mechanoreceptors. *Neurosci Biobehav Rev, 61*, 225-238. doi:10.1016/j.neubiorev.2015.12.009

DosSantos, M. F., Moura, B. S., & DaSilva, A. F. (2017). Reward Circuitry Plasticity in Pain Perception and Modulation. *Front Pharmacol, 8*, 790. doi:10.3389/fphar.2017.00790

Dostrovsky, J. O., & Craig, A. D. (1996). Cooling-specific spinothalamic neurons in the monkey. *J Neurophysiol, 76*(6), 3656-3665. doi:10.1152/jn.1996.76.6.3656

Dubner, R., Sessle, B. J., & Storey, A. T. (1978). The Neural Basis of Oral and Facial Function. *New York: Plenum*.

Dueñas, M., Ojeda, B., Salazar, A., Mico, J. A., & Failde, I. (2016). A review of chronic pain impact on patients, their social environment and the health care system. *Journal of pain research, 9*, 457.

Dutta, S., Beaver, J., Halcomb, C. J., & Jasnow, A. M. (2021). Dissociable roles of the nucleus accumbens core and shell subregions in the expression and extinction of conditioned fear. *Neurobiol Stress, 15*, 100365. doi:10.1016/j.ynstr.2021.100365

Elman, I., & Borsook, D. (2018). Threat Response System: Parallel Brain Processes in Pain vis-a-vis Fear and Anxiety. *Front Psychiatry, 9*, 29. doi:10.3389/fpsyt.2018.00029

Enck, P., Bingel, U., Schedlowski, M., & Rief, W. (2013). The placebo response in medicine: minimize, maximize or personalize? *Nat Rev Drug Discov, 12*(3), 191-204. doi:10.1038/nrd3923

Etkin, A., Buchel, C., & Gross, J. J. (2015). The neural bases of emotion regulation. *Nat Rev Neurosci, 16*(11), 693-700. doi:10.1038/nrn4044

Fields, H. L. (2018). How expectations influence pain. *Pain, 159*, S3-S10.

Fischl, B. (2012). FreeSurfer. *Neuroimage, 62*(2), 774-781. doi:10.1016/j.neuroimage.2012.01.021

Floresco, S. B. (2015). The nucleus accumbens: an interface between cognition, emotion, and action. *Annu Rev Psychol, 66*, 25-52. doi:10.1146/annurev-psych-010213-115159

Francis, T. C., & Lobo, M. K. (2017). Emerging role for nucleus accumbens medium spiny neuron subtypes in depression. *Biological psychiatry, 81*(8), 645-653.

Galer, B. S., & Jensen, M. P. (1997). Development and preliminary validation of a pain measure specific to neuropathic pain: the Neuropathic Pain Scale. *Neurology, 48*(2), 332-338. doi:10.1212/wnl.48.2.332

Groenewegen, H. J., Berendse, H. W., & Haber, S. N. (1993). Organization of the output of the ventral striatopallidal system in the rat: ventral pallidal efferents. *Neuroscience, 57*(1), 113-142. doi:10.1016/0306-4522(93)90115-v

Hagerty, M. R., Isaacs, J., Brasington, L., Shupe, L., Fetz, E. E., & Cramer, S. C. (2013). Case study of ecstatic meditation: fMRI and EEG evidence of self-stimulating a reward system. *Neural Plast, 2013*, 653572. doi:10.1155/2013/653572

Hamel, L., Thangarasa, T., Samadi, O., & Ito, R. (2017). Caudal Nucleus Accumbens Core Is Critical in the Regulation of Cue-Elicited Approach-Avoidance Decisions. *eNeuro, 4*(1). doi:10.1523/ENEURO.0330-16.2017

Harden, R. N., Weinland, S. R., Remble, T. A., Houle, T. T., Colio, S., Steedman, S., . . . American Pain Society, P. (2005). Medication Quantification Scale Version III: update in medication classes and revised detriment weights by survey of American Pain Society Physicians. *J Pain, 6*(6), 364-371. doi:10.1016/j.jpain.2005.01.350

Harris, H. N., & Peng, Y. B. (2020). Evidence and explanation for the involvement of the nucleus accumbens in pain processing. *Neural Regen Res, 15*(4), 597-605. doi:10.4103/1673-5374.266909

Hart, A. S., Rutledge, R. B., Glimcher, P. W., & Phillips, P. E. (2014). Phasic dopamine release in the rat nucleus accumbens symmetrically encodes a reward prediction error term. *J Neurosci, 34*(3), 698-704. doi:10.1523/JNEUROSCI.2489-13.2014

Hashmi, J. A., Baliki, M. N., Huang, L., Baria, A. T., Torbey, S., Hermann, K. M., . . . Apkarian, A. V. (2013). Shape shifting pain: chronification of back pain shifts brain representation from nociceptive to emotional circuits. *Brain, 136*(Pt 9), 2751-2768. doi:10.1093/brain/awt211

Hashmi, J. A., & Davis, K. D. (2008). Effect of static and dynamic heat pain stimulus profiles on the temporal dynamics and interdependence of pain qualities, intensity, and affect. *Journal of neurophysiology, 100*(4), 1706-1715.

Hashmi, J. A., & Davis, K. D. (2009). Women experience greater heat pain adaptation and habituation than men. *Pain, 145*(3), 350-357.

Hashmi, J. A., Loggia, M. L., Khan, S., Gao, L., Kim, J., Napadow, V., . . . Akeju, O. (2017). Dexmedetomidine Disrupts the Local and Global Efficiencies of Large-scale Brain Networks. *Anesthesiology, 126*(3), 419-430. doi:10.1097/ALN.0000000000001509

Hauser, T. U., Eldar, E., & Dolan, R. J. (2017). Separate mesocortical and mesolimbic pathways encode effort and reward learning signals. *Proc Natl Acad Sci U S A, 114*(35), E7395-E7404. doi:10.1073/pnas.1705643114

Heimer, L., Zahm, D. S., Churchill, L., Kalivas, P. W., & Wohltmann, C. (1991). Specificity in the projection patterns of accumbal core and shell in the rat. *Neuroscience, 41*(1), 89-125. doi:10.1016/0306-4522(91)90202-y

Ikemoto, S., & Panksepp, J. (1999). The role of nucleus accumbens dopamine in motivated behavior: a unifying interpretation with special reference to reward-seeking. *Brain Res Brain Res Rev, 31*(1), 6-41. doi:10.1016/s0165-0173(99)00023-5

Jenkinson, M., Beckmann, C. F., Behrens, T. E., Woolrich, M. W., & Smith, S. M. (2012). Fsl. *Neuroimage, 62*(2), 782-790. doi:10.1016/j.neuroimage.2011.09.015

Kai, Y., Li, Y., Sun, T., Yin, W., Mao, Y., Li, J., . . . Li, J. (2018). A medial prefrontal cortex-nucleus acumens corticotropin-releasing factor circuitry for neuropathic pain-increased susceptibility to opioid reward. *Translational Psychiatry, 8*(1), 1-12.

Kalivas, P. W., & Duffy, P. (1995). Selective activation of dopamine transmission in the shell of the nucleus accumbens by stress. *Brain research, 675*(1-2), 325-328.

Katz, J., Rosenbloom, B. N., & Fashler, S. (2015). Chronic Pain, Psychopathology, and DSM-5 Somatic Symptom Disorder. *Can J Psychiatry, 60*(4), 160-167. doi:10.1177/070674371506000402

Kim, H., Nanavaty, N., Ahmed, H., Mathur, V. A., & Anderson, B. A. (2021). Motivational Salience Guides Attention to Valuable and Threatening Stimuli: Evidence from Behavior and Functional Magnetic Resonance Imaging. *J Cogn Neurosci, 33*(12), 2440-2460. doi:10.1162/jocn_a_01769

Knutson, B., Wimmer, G. E., Kuhnen, C. M., & Winkielman, P. (2008). Nucleus accumbens activation mediates the influence of reward cues on financial risk taking. *NeuroReport, 19*(5), 509-513.

Kober, H., Barrett, L. F., Joseph, J., Bliss-Moreau, E., Lindquist, K., & Wager, T. D. (2008). Functional grouping and cortical-subcortical interactions in emotion: a meta-analysis of neuroimaging studies. *Neuroimage, 42*(2), 998-1031. doi:10.1016/j.neuroimage.2008.03.059

Kong, J., Jensen, K., Loiotile, R., Cheetham, A., Wey, H.-Y., Tan, Y., . . . Gollub, R. L. (2013). Functional connectivity of the frontoparietal network predicts cognitive modulation of pain. *PAIN®, 154*(3), 459-467.

Koyama, M. S., O'Connor, D., Shehzad, Z., & Milham, M. P. (2017). Differential contributions of the middle frontal gyrus functional connectivity to literacy and numeracy. *Sci Rep, 7*(1), 17548. doi:10.1038/s41598-017-17702-6

Kutlu, M. G., Zachry, J. E., Melugin, P. R., Cajigas, S. A., Chevee, M. F., Kelly, S. J., . . . Calipari, E. S. (2021). Dopamine release in the nucleus accumbens core signals perceived saliency. *Curr Biol, 31*(21), 4748-4761 e4748. doi:10.1016/j.cub.2021.08.052

LeDoux, J., & Daw, N. D. (2018). Surviving threats: neural circuit and computational implications of a new taxonomy of defensive behaviour. *Nat Rev Neurosci, 19*(5), 269-282. doi:10.1038/nrn.2018.22

Lee, M., Manders, T. R., Eberle, S. E., Su, C., D'Amour, J., Yang, R., . . . Wang, J. (2015). Activation of corticostriatal circuitry relieves chronic neuropathic pain. *J Neurosci, 35*(13), 5247-5259. doi:10.1523/JNEUROSCI.3494-14.2015

Lele, P. P., Sinclair, D. C., & Weddell, G. (1954). The reaction time to touch. *J Physiol, 123*(1), 187-203. doi:10.1113/jphysiol.1954.sp005042

Li, L., Mi, Y., Zhang, W., Wang, D. H., & Wu, S. (2018). Dynamic Information Encoding With Dynamic Synapses in Neural Adaptation. *Front Comput Neurosci, 12*, 16. doi:10.3389/fncom.2018.00016

Li, S. S., & McNally, G. P. (2015). A role of nucleus accumbens dopamine receptors in the nucleus accumbens core, but not shell, in fear prediction error. *Behav Neurosci, 129*(4), 450-456. doi:10.1037/bne0000071

Lim, M., O'Grady, C., Cane, D., Goyal, A., Lynch, M., Beyea, S., & Hashmi, J. A. (2020). Threat Prediction from Schemas as a Source of Bias in Pain Perception. *J Neurosci, 40*(7), 1538-1548. doi:10.1523/JNEUROSCI.2104-19.2019

Liu, S., Erkkinen, M. G., Healey, M. L., Xu, Y., Swett, K. E., Chow, H. M., & Braun, A. R. (2015). Brain activity and connectivity during poetry composition: Toward a multidimensional model of the creative process. *Hum Brain Mapp, 36*(9), 3351-3372. doi:10.1002/hbm.22849

Lorenz, J., Minoshima, S., & Casey, K. L. (2003). Keeping pain out of mind: the role of the dorsolateral prefrontal cortex in pain modulation. *Brain, 126*(Pt 5), 1079-1091. doi:10.1093/brain/awg102

Loriaux, A. L., Roitman, J. D., & Roitman, M. F. (2011). Nucleus accumbens shell, but not core, tracks motivational value of salt. *J Neurophysiol, 106*(3), 1537-1544. doi:10.1152/jn.00153.2011

MacIver, M. B., & Tanelian, D. L. (1993). Structural and functional specialization of A delta and C fiber free nerve endings innervating rabbit corneal epithelium. *J Neurosci, 13*(10), 4511-4524. Retrieved from https://www.ncbi.nlm.nih.gov/pubmed/8410200

Madsen, C. S., Johnsen, B., Fuglsang-Frederiksen, A., Jensen, T. S., & Finnerup, N. B. (2012). Increased contact heat pain and shortened latencies of contact heat evoked potentials following capsaicin-induced heat hyperalgesia. *Clin Neurophysiol, 123*(7), 1429-1436. doi:10.1016/j.clinph.2011.11.032

Makary, M. M., Polosecki, P., Cecchi, G. A., DeAraujo, I. E., Barron, D. S., Constable, T. R., . . . Geha, P. (2020). Loss of nucleus accumbens low-frequency fluctuations is a signature of chronic pain. *Proc Natl Acad Sci U S A, 117*(18), 10015-10023. doi:10.1073/pnas.1918682117

Mandrekar, J. N. (2010). Receiver operating characteristic curve in diagnostic test assessment. *J Thorac Oncol, 5*(9), 1315-1316. doi:10.1097/JTO.0b013e3181ec173d

Mason, M. F., Norton, M. I., Van Horn, J. D., Wegner, D. M., Grafton, S. T., & Macrae, C. N. (2007). Wandering minds: the default network and stimulus-independent thought. *Science, 315*(5810), 393-395. doi:10.1126/science.1131295

Mayr, A., Jahn, P., Stankewitz, A., Deak, B., Winkler, A., Witkovsky, V., . . . Schulz, E. (2022). Patients with chronic pain exhibit individually unique cortical signatures of pain encoding. *Hum Brain Mapp, 43*(5), 1676-1693. doi:10.1002/hbm.25750

Melzack, R. (1987). The short-form McGill Pain Questionnaire. *Pain, 30*(2), 191-197. doi:10.1016/0304-3959(87)91074-8

Melzack, R., & Casey, K. L. (1967). Localized temperature changes evoked in the brain by somatic stimulation. *Exp Neurol, 17*(3), 276-292. doi:10.1016/0014-4886(67)90107-0

Melzack, R., & Wall, P. D. (1965). Pain mechanisms: a new theory. *Science, 150*(3699), 971-979. doi:10.1126/science.150.3699.971

Moayedi, M., & Davis, K. D. (2013). Theories of pain: from specificity to gate control. *Journal of neurophysiology, 109*(1), 5-12.

Moulin, D. E., Clark, A. J., Speechley, M., & Morley-Forster, P. K. (2002). Chronic pain in Canada-prevalence, treatment, impact and the role of opioid analgesia. *Pain Research and Management, 7*(4), 179-184.

Mountcastle, V. B., & Darian-Smith, I. (1968). Neural mechanisms in somesthesia. *Medical physiology, 2*, 1372-1423.

Muthulingam, J., Olesen, S. S., Hansen, T. M., Seminowicz, D. A., Burrowes, S., Drewes, A. M., & Frøkjær, J. B. (2018). Progression of structural brain changes in patients with chronic pancreatitis and its association to chronic pain: a 7-year longitudinal follow-up study. *Pancreas, 47*(10), 1267-1276.

Nachev, P., Lopez-Sosa, F., Gonzalez-Rosa, J. J., Galarza, A., Avecillas, J., Pineda-Pardo, J. A., . . . Strange, B. (2015). Dynamic risk control by human nucleus accumbens. *Brain, 138*(12), 3496-3502.

O'Reilly, R. C. (2010). The What and How of prefrontal cortical organization. *Trends Neurosci, 33*(8), 355-361. doi:10.1016/j.tins.2010.05.002

Okano, H., Hirano, T., & Balaban, E. (2000). Learning and memory. *Proc Natl Acad Sci U S A, 97*(23), 12403-12404. doi:10.1073/pnas.210381897

Panneton, W. M., Gan, Q., & Ariel, M. (2015). Injections of Algesic Solutions into Muscle Activate the Lateral Reticular Formation: A Nociceptive Relay of the Spinoreticulothalamic Tract. *PLoS One, 10*(7), e0130939. doi:10.1371/journal.pone.0130939

Patestas, M. A., & Gartner, L. P. (2016). *A textbook of neuroanatomy*: John Wiley & Sons.

Perl, E. R. (2007). Ideas about pain, a historical view. *Nature Reviews Neuroscience, 8*(1), 71-80.

Philiastides, M. G., Auksztulewicz, R., Heekeren, H. R., & Blankenburg, F. (2011). Causal role of dorsolateral prefrontal cortex in human perceptual decision making. *Curr Biol, 21*(11), 980-983. doi:10.1016/j.cub.2011.04.034

Phillips, C. (2014). PAIN IN CANADA FACT SHEET. Retrieved from http://www.chronicpaintoronto.com/wp-content/uploads/2016/06/pain_fact_sheet_en.pdf

Piantadosi, P. T., Yeates, D. C., & Floresco, S. B. (2018). Cooperative and dissociable involvement of the nucleus accumbens core and shell in the promotion and inhibition of actions during active and inhibitory avoidance. *Neuropharmacology, 138*, 57-71.

Pittenger, C., & Duman, R. S. (2008). Stress, depression, and neuroplasticity: a convergence of mechanisms. *Neuropsychopharmacology, 33*(1), 88-109. doi:10.1038/sj.npp.1301574

Power, J. D., Barnes, K. A., Snyder, A. Z., Schlaggar, B. L., & Petersen, S. E. (2012). Spurious but systematic correlations in functional connectivity MRI networks arise from subject motion. *Neuroimage, 59*(3), 2142-2154. doi:10.1016/j.neuroimage.2011.10.018

Raja, S. N., Carr, D. B., Cohen, M., Finnerup, N. B., Flor, H., Gibson, S., . . . Sluka, K. A. (2020). The revised IASP definition of pain: Concepts, challenges, and compromises. *Pain, 161*(9), 1976.

Ray, M. H., Moaddab, M., & McDannald, M. A. (2021). Distinct threat and valence signals in rat nucleus accumbens core. *bioRxiv*, 2021.2005.2027.446063. doi:10.1101/2021.05.27.446063

Ray, M. H., Moaddab, M., & McDannald, M. A. (2022). Threat and Bidirectional Valence Signaling in the Nucleus Accumbens Core. *J Neurosci, 42*(5), 817-833. doi:10.1523/JNEUROSCI.1107-21.2021

Ray, M. H., Russ, A. N., Walker, R. A., & McDannald, M. A. (2020). The nucleus accumbens core is necessary to scale fear to degree of threat. *Journal of Neuroscience, 40*(24), 4750-4760.

Rexed, B. (1952). The cytoarchitectonic organization of the spinal cord in the cat. *J Comp Neurol, 96*(3), 414-495. doi:10.1002/cne.900960303

Saddoris, M. P., Cacciapaglia, F., Wightman, R. M., & Carelli, R. M. (2015). Differential dopamine release dynamics in the nucleus accumbens core and shell reveal complementary signals for error prediction and incentive motivation. *Journal of Neuroscience, 35*(33), 11572-11582.

Saghayi, M., Greenberg, J., O'Grady, C., Varno, F., Hashmi, M. A., Bracken, B., . . . Hashmi, J. A. (2020). Brain network topology predicts participant adherence to mental training programs. *Netw Neurosci, 4*(3), 528-555. doi:10.1162/netn_a_00136

Salgado, S., & Kaplitt, M. G. (2015). The Nucleus Accumbens: A Comprehensive Review. *Stereotact Funct Neurosurg, 93*(2), 75-93. doi:10.1159/000368279

Schultz, W., Dayan, P., & Montague, P. R. (1997). A neural substrate of prediction and reward. *Science, 275*(5306), 1593-1599.

Seeley, W. W. (2019). The Salience Network: A Neural System for Perceiving and Responding to Homeostatic Demands. *J Neurosci, 39*(50), 9878-9882. doi:10.1523/JNEUROSCI.1138-17.2019

Segerdahl, A. R., Mezue, M., Okell, T. W., Farrar, J. T., & Tracey, I. (2015). The dorsal posterior insula subserves a fundamental role in human pain. *Nat Neurosci, 18*(4), 499-500. doi:10.1038/nn.3969

Seminowicz, D. A., & Moayedi, M. (2017). The Dorsolateral Prefrontal Cortex in Acute and Chronic Pain. *J Pain, 18*(9), 1027-1035. doi:10.1016/j.jpain.2017.03.008

Seymour, B. (2019). Pain: A Precision Signal for Reinforcement Learning and Control. *Neuron, 101*(6), 1029-1041. doi:10.1016/j.neuron.2019.01.055

Shih, Y. W., Tsai, H. Y., Lin, F. S., Lin, Y. H., Chiang, C. Y., Lu, Z. L., & Tseng, M. T. (2019). Effects of Positive and Negative Expectations on Human Pain Perception Engage Separate But Interrelated and Dependently Regulated Cerebral Mechanisms. *J Neurosci, 39*(7), 1261-1274. doi:10.1523/JNEUROSCI.2154-18.2018

Shulman, G. L., Astafiev, S. V., Franke, D., Pope, D. L., Snyder, A. Z., McAvoy, M. P., & Corbetta, M. (2009). Interaction of stimulus-driven reorienting and expectation in ventral and dorsal frontoparietal and basal ganglia-cortical networks. *J Neurosci, 29*(14), 4392-4407. doi:10.1523/JNEUROSCI.5609-08.2009

Shupler, M. S., Kramer, J. K., Cragg, J. J., Jutzeler, C. R., & Whitehurst, D. G. (2019). Pan-Canadian estimates of chronic pain prevalence from 2000 to 2014: a repeated cross-sectional survey analysis. *The Journal of Pain, 20*(5), 557-565.

Simon, L. S. (2012). Relieving pain in America: A blueprint for transforming prevention, care, education, and research. *Journal of pain & palliative care pharmacotherapy, 26*(2), 197-198.

Sinclair, D. C. (1955). Cutaneous sensation and the doctrine of specific energy. *Brain, 78*(4), 584-614. doi:10.1093/brain/78.4.584

Smith, S. M., Vidaurre, D., Beckmann, C. F., Glasser, M. F., Jenkinson, M., Miller, K. L., . . . Van Essen, D. C. (2013). Functional connectomics from resting-state fMRI. *Trends Cogn Sci, 17*(12), 666-682. doi:10.1016/j.tics.2013.09.016

Sokol-Hessner, P., Hutcherson, C., Hare, T., & Rangel, A. (2012). Decision value computation in DLPFC and VMPFC adjusts to the available decision time. *Eur J Neurosci, 35*(7), 1065-1074. doi:10.1111/j.1460-9568.2012.08076.x

Spicer, J., Galvan, A., Hare, T. A., Voss, H., Glover, G., & Casey, B. (2007). Sensitivity of the nucleus accumbens to violations in expectation of reward. *Neuroimage, 34*(1), 455-461.

Spielberger, C. (2010). State-trait anxiety inventory. The Corsini encyclopedia of psychology. *Hoboken: Wiley, 1*.

Spreng, R. N., Mar, R. A., & Kim, A. S. (2009). The common neural basis of autobiographical memory, prospection, navigation, theory of mind, and the default mode: a quantitative meta-analysis. *J Cogn Neurosci, 21*(3), 489-510. doi:10.1162/jocn.2008.21029

Spreng, R. N., Stevens, W. D., Chamberlain, J. P., Gilmore, A. W., & Schacter, D. L. (2010). Default network activity, coupled with the frontoparietal control network, supports goal-directed cognition. *Neuroimage, 53*(1), 303-317. doi:10.1016/j.neuroimage.2010.06.016

Stopper, C. M., & Floresco, S. B. (2011). Contributions of the nucleus accumbens and its subregions to different aspects of risk-based decision making. *Cogn Affect Behav Neurosci, 11*(1), 97-112. doi:10.3758/s13415-010-0015-9

Sullivan, M. B. S. P. J. (1995). The Pain Catastrophizing Scale: Development and validation. *Psychol Assessment, 7*(4), 524-532.

Sunavsky, A., & Poppenk, J. (2020). Neuroimaging predictors of creativity in healthy adults. *Neuroimage, 206*, 116292. doi:10.1016/j.neuroimage.2019.116292

Tracey, W. D., Jr. (2017). Nociception. *Curr Biol, 27*(4), R129-R133. doi:10.1016/j.cub.2017.01.037

Vachon-Presseau, E., Tétreault, P., Petre, B., Huang, L., Berger, S. E., Torbey, S., . . . Griffith, J. W. (2016). Corticolimbic anatomical characteristics predetermine risk for chronic pain. *Brain, 139*(7), 1958-1970.

Vase, L., Vollert, J., Finnerup, N. B., Miao, X., Atkinson, G., Marshall, S., . . . Segerdahl, M. (2015). Predictors of the placebo analgesia response in randomized controlled trials of chronic pain: a meta-analysis of the individual data from nine industrially sponsored trials. *Pain, 156*(9), 1795-1802. doi:10.1097/j.pain.0000000000000217

Ventura, R., Morrone, C., & Puglisi-Allegra, S. (2007). Prefrontal/accumbal catecholamine system determines motivational salience attribution to both reward- and aversion-related stimuli. *Proc Natl Acad Sci U S A, 104*(12), 5181-5186. doi:10.1073/pnas.0610178104

Vossel, S., Geng, J. J., & Fink, G. R. (2014). Dorsal and ventral attention systems: distinct neural circuits but collaborative roles. *Neuroscientist, 20*(2), 150-159. doi:10.1177/1073858413494269

Wager, T. D., Davidson, M. L., Hughes, B. L., Lindquist, M. A., & Ochsner, K. N. (2008). Prefrontal-subcortical pathways mediating successful emotion regulation. *Neuron, 59*(6), 1037-1050. doi:10.1016/j.neuron.2008.09.006

Wang, S., Veinot, J., Goyal, A., Khatibi, A., Lazar, S. W., & Hashmi, J. A. (2022). Distinct networks of periaqueductal gray columns in pain and threat processing. *Neuroimage, 250*, 118936. doi:10.1016/j.neuroimage.2022.118936

Wei, S. Y., Chao, H. T., Tu, C. H., Li, W. C., Low, I., Chuang, C. Y., . . . Hsieh, J. C. (2016). Changes in functional connectivity of pain modulatory systems in women with primary dysmenorrhea. *Pain, 157*(1), 92-102. doi:10.1097/j.pain.0000000000000340

Wenzel, J. M., Rauscher, N. A., Cheer, J. F., & Oleson, E. B. (2015). A role for phasic dopamine release within the nucleus accumbens in encoding aversion: a review of the neurochemical literature. *ACS Chem Neurosci, 6*(1), 16-26. doi:10.1021/cn500255p

West, E. A., & Carelli, R. M. (2016). Nucleus Accumbens Core and Shell Differentially Encode Reward-Associated Cues after Reinforcer Devaluation. *J Neurosci, 36*(4), 1128-1139. doi:10.1523/JNEUROSCI.2976-15.2016

Willis, W. D., & Westlund, K. N. (1997). Neuroanatomy of the pain system and of the pathways that modulate pain. *J Clin Neurophysiol, 14*(1), 2-31. doi:10.1097/00004691-199701000-00002

Xia, M., Wang, J., & He, Y. (2013). BrainNet Viewer: a network visualization tool for human brain connectomics. *PLoS One, 8*(7), e68910. doi:10.1371/journal.pone.0068910

Xia, S. H., Yu, J., Huang, X., Sesack, S. R., Huang, Y. H., Schluter, O. M., . . . Dong, Y. (2020). Cortical and Thalamic Interaction with Amygdala-to-Accumbens Synapses. *J Neurosci, 40*(37), 7119-7132. doi:10.1523/JNEUROSCI.1121-20.2020

Xia, X., Fan, L., Cheng, C., Eickhoff, S. B., Chen, J., Li, H., & Jiang, T. (2017). Multimodal connectivity-based parcellation reveals a shell-core dichotomy of the human nucleus accumbens. *Hum Brain Mapp, 38*(8), 3878-3898. doi:10.1002/hbm.23636

Yam, M. F., Loh, Y. C., Tan, C. S., Khadijah Adam, S., Abdul Manan, N., & Basir, R. (2018). General Pathways of Pain Sensation and the Major Neurotransmitters Involved in Pain Regulation. *Int J Mol Sci, 19*(8). doi:10.3390/ijms19082164

Yeomans, D. C., Pirec, V., & Proudfit, H. K. (1996). Nociceptive responses to high and low rates of noxious cutaneous heating are mediated by different nociceptors in the rat: behavioral evidence. *Pain, 68*(1), 133-140.

Yezierski, R. P. (1990). Effects of midbrain and medullary stimulation on spinomesencephalic tract cells in the cat. *J Neurophysiol, 63*(2), 240-255. doi:10.1152/jn.1990.63.2.240

Zahm, D. S. (2000). An integrative neuroanatomical perspective on some subcortical substrates of adaptive responding with emphasis on the nucleus accumbens. *Neuroscience & Biobehavioral Reviews, 24*(1), 85-105.

Zahm, D. S., Williams, E., & Wohltmann, C. (1996). Ventral striatopallidothalamic projection: IV. Relative involvements of neurochemically distinct subterritories in the ventral pallidum and adjacent parts of the rostroventral forebrain. *J Comp Neurol, 364*(2), 340-362. doi:10.1002/(SICI)1096-9861(19960108)364:2<340::AID-CNE11>3.0.CO;2-T

Zhang, Y., Zhu, Y., Cao, S. X., Sun, P., Yang, J. M., Xia, Y. F., . . . Li, X. M. (2020). MeCP2 in cholinergic interneurons of nucleus accumbens regulates fear learning. *Elife, 9*. doi:10.7554/eLife.55342

Zhou, H., Martinez, E., Lin, H. H., Yang, R., Dale, J. A., Liu, K., . . . Wang, J. (2018). Inhibition of the prefrontal projection to the nucleus accumbens enhances pain sensitivity and affect. *Frontiers in cellular neuroscience*, 240.